Comprehensive studies on functional expression of *OsGAD4* gene in rice plants and physiological analysis of its genome-edited mutants under abiotic stress conditions

イネにおける *OsGAD4* 遺伝子の機能発現と非生物的ストレス下でのそのゲノム編集変異体の生理学的解析に関する総合研究

A Dissertation
Presented to the Graduate School of Natural Science and Technology
of Shimane University

in Partial Fulfilment of the Requirements for the Degree

Doctor of Philosophy in Science
(Doctoral Program in Science and Engineering for Innovation)

By
NADIA AKTER
N21D208

August 2024

Thesis Supervisor:
Professor Kazuhito Akama

Co-supervisors:
Professor Yuuki Kodama
Associate Professor Kohji Nishimura
Associate Professor Sadanobu Katoh

Acknowledgments

I wish to express my sincere gratitude and intense appreciation to my supervisor Professor Dr. KAZUHITO AKAMA for allowing me to conduct my research and study under his intellectual supervision. It would be almost impossible for me to complete the dissertation without his valuable guidance and continuous encouragement. I do acknowledge his kind support throughout my stay period in Japan.

I also want to express my whole-hearted thanks to my co-supervisors YUUKI KODAMA, KOHJI NISHIMURA and SADANOBU KATOH for their cordial advice and support during this research. In addition, I extend my gratefulness to all the laboratory colleagues for their team effort, friendly behavior, and enjoyable working environment.

I express my boundless gratitude and endless thanks to my parents, my daughter, my husband, and other family members for their immense love, sacrifice, and patience which can never be repaid. During the challenging times of the COVID-19 pandemic, it was my beloved family who inspired me profoundly to continue studying abroad. Their unwavering support, resilience, and encouragement were like a beacon of light, guiding me through the uncertainties and difficulties of those turbulent times, for which I am deeply grateful.

I am indebted to the Japanese Government (Monbukagakusho: MEXT) Scholarship for supporting my study and livelihood during the whole period. I am thankful to my employer Bangladesh Rice Research Institute for allowing me to study at Shimane University in Japan. Finally, it is my creator Almighty Allah, the most Merciful who blessed me with the strength to carry out my study to its conclusion.

NADIA AKTER

Abbreviations

GABA =γ-Aminobutyric acid
α- KG= α-ketoglutarate
GAD= Glutamate decarboxylase
SSA= Succinic semialdehyde
GHB= Gamma hydroxybutyric acid
GLYR= Glyoxylate Reductase
GABA-T= GABA transaminase
SSADH= Succinic semialdehyde dehydrogenase
SSR= Succinic semialdehyde reductase
CaM=Calmodulin
CaMBD =Calmodulin Binding Domain
TCA=Tricarboxylic acid
CRISPR =Clustered regularly interspaced short palindromic repeats
ZFN =Zinc-finger nucleases
TALEN =Transcription activator-like effector nucleases
DSB =double strand break
HR=homologous recombination
NHEJ =Non-homologous end joining
PAM =Protospacer adjacent motif
sgRNA =single guide RNA
HPT= Hygromycin phosphotransferase
Spe= Spectinomycin
MS=Murashige and skoog
CTAB =Cetyltrimethylammonium bromide
RT-qPCR=Reverse transcription-quantitative polymerase chain reaction
GC/MS= Gas chromatography/ mass spectrometry
CAT= Catalase
POD=Peroxidase
APX=Ascorbate peroxidase
DEG= Differentially Expressed Genes
GO= Gene Ontology
KEGG= Kyoto Encyclopedia of Genes and Genomes

Table of Contents

Chapter II. Production of GABA-fortified rice through CRISPR/Cas9 genome editing

Chapter III. Evaluation of abiotic stress tolerance of truncated mutant

List of Figures

List of Tables

Chapter I: General Introduction

1.1 Rice, as a crop of major importance

We are living on a planet where rice (*Oryza sativa* L.) contributes as a staple food for the lion's share of its inhabitants. People in most Asian nations consume rice as their major diet. In 20022/23, worldwide rice production was recorded as 519.5 million tonnes, while per capita consumption was 53.9 kg/yr (FAO, 2022). Bearing in mind the ever-increasing demand for rice, nutritional improvements of this species may have a great impact on the human population. In addition to its contribution as a principal cereal, the rice plant is serving as a model plant for molecular-level study because of its known genome size and composition. However, in recent years, climate change has been taking a toll on living organisms i.e. flora and fauna. Climate change is exerting pressure on agriculture, making it more difficult to produce adequate food (IPCC, 2022). Plants have been experiencing many stressors due to adverse climatic conditions, including waterlogging, drought, heat, cold, and salt. Frequent stresses are affecting crops, particularly rice cultivation and therefore threatening food security.

1.2 GABA and its beneficial effect

Gamma-aminobutyric acid (GABA) is a four-carbon, non-proteinous amino acid (Fig. 1), universally found in prokaryotic and eukaryotic organisms (Satya et al., 1990; Shelp et al., 1999). The first report on the identification of GABA in potato tuber tissue was disclosed in 1949 (Steward et al., 1949).

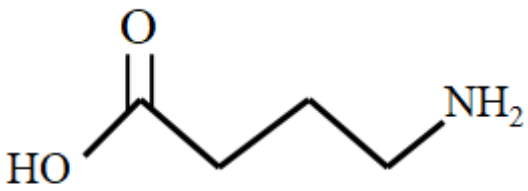

Figure 1. Chemical structure of GABA ($C_4H_9NO_2$). It is mostly found as zwitterions; with the carboxyl group deprotonated, and the amino group protonated.

GABA is regarded as a beneficial and healthful substance. It is stated to have a significant inhibitory neurotransmitter role in the central nervous system of animals (Curtis et al., 1974). GABA has been used in a broad variety of discomforts due to its function as an inhibitory neurotransmitter and its general availability. Chronic stress (Jie et al., 2018), anxiety disorders (Nemeroff, 2003), sleep abnormalities including insomnia (Gottesmann, 2002), and the diagnosis and treatment of acute and chronic pressure have all been linked to low levels of GABA or reduced GABA activity. GABA may be found in a variety of foods that are naturally occurring, including tea, tomatoes, beans, sprouted whole grains (germinated brown rice), and several fermented foods that can be consumed as part of a normal diet (Diana et al., 2014; Rashmi et al., 2018). Naturally occurring food sources do not

provide enough GABA to prevent lifestyle-related disorders; thus, foods enhanced with GABA are required to have a health-promoting impact (Park et al., 2007; Yamakoshi et al., 2007).

The investigation on GABA in natural foods has been performed mostly with germinated brown rice (GBR). Brown rice in usual form contains a small quantity of GABA, but germination increases its GABA content by the inherent synthesis. Significant accumulation of GABA was reported in the rice germ during water soaking (Saikusa et al., 1994). Moreover, it was reported that physical stress during germination such as temperature manipulation and oxygen deficiency might enhance the GABA synthesis in GBR (Ohtsubo et al., 2005). The repeated soaking and gaseous treatment of brown rice kernels also accelerated the GABA synthesis during germination (Komatsuzaki et al., 2007; Thitinunsomboon et al., 2013). Besides, GABA functions as an endogenous signaling molecule in plant development and growth control in addition to its metabolic function (Carillo 2018, Fait et al., 2008; Renault et al., 2011).

1.3 GABA metabolism in plants

Glutamate controls the primary pathway of GABA synthesis through the activity of the cytosolic enzyme glutamate decarboxylase (GAD) (Shelp et al., 2012), whereas polyamine breakdown provides an alternate mechanism (Yang et al., 2015).

When glutamate dehydrogenase (GDH) is present in the cytosol, α-ketoglutarate is aminated to glutamate. GABA is predominantly produced in the cytosol from glutamate by an irreversible decarboxylation process that is catalyzed by glutamate decarboxylase (GAD). It is transported to the mitochondria and converted into succinic semialdehyde and then catabolized into succinate by succinic semialdehyde dehydrogenase (SSADH) and GABA transaminase (GABA-T) (Bown et al., 1997). This succinate, or succinic acid, rejoins the TCA cycle. GABA shunt is the term used to describe this route (Fig. 2).

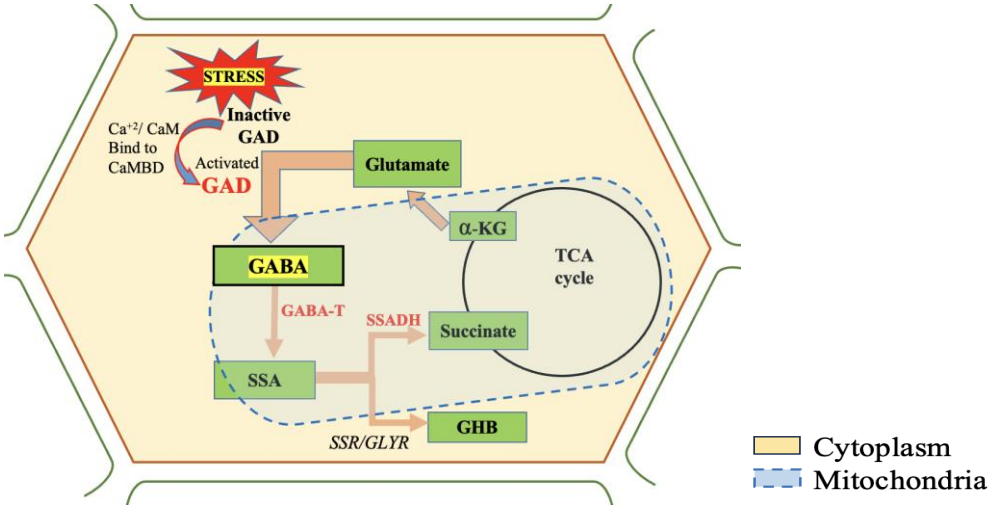

Figure 2. GABA metabolism in plants.

α- KG= α-ketoglutarate, GAD= Glutamate decarboxylase, CaMBD= Calmodulin binding domain, SSA= Succinic semialdehyde, GABA-T= GABA transaminase, SSADH= Succinic semialdehyde

dehydrogenase, GHB= Gamma hydroxy butyrate, SSR= Succinic semialdehyde reductase, GLYR= Glyoxylate reductase.

During normal conditions, plant cells produce a basal amount of GABA. However, when the plant is exposed to stress conditions, GAD is stimulated by a Ca^{2+}/CaM-dependent reaction. Thus, the activated GAD leads to increased synthesis of GABA from glutamate.

1.4 Major elements associated with GABA shunt

1.4.1 Glutamate decarboxylase (GAD) and Calmodulin Binding Domain (CaMBD)

An essential enzyme that converts glutamate into GABA is called GAD. This makes it one of the GABA pathway enzymes that has been well-researched. The cloning of the petunia *GAD* gene and the identification of the encoded enzyme as a Ca^{2+}-dependent calmodulin (CaM)-binding protein have sparked research into the role of GAD and its regulation in plants (Baum et al., 1993). Group II decarboxylases are PLP-dependent enzymes. The plant and bacterial proteins exhibit notable similarities in terms of sequence identity and conformation (Gut et al., 2009). Plant GAD polypeptides are 43–62 kDa subunits that appear to be dimeric or hexameric in their natural shape (Shelp et al., 2012b). Nevertheless, following genebank searches, the GAD genes of a few plant species were discovered to exhibit extremely varied CaM-binding sites. These plant species include five GADs in Arabidopsis, rice, tomato, and maize, nine GADs in soybeans, and six GADs in poplar. (Shelp et al., 1999; Akihiro et al., 2008).

Later, it was discovered that Ca^{2+}-CaM induces GAD activity in extracts from a variety of plant species. A comprehensive molecular examination of the petunia GAD CaM-binding domain (Arazi et al., 1995) and the identification of the refined recombinant protein as an enzyme controlled by Ca^{2+}-CaM (Snedden et al., 1996) yielded a functional model that elucidated the rapid increase of GAD activity in reaction to diverse stress scenarios. This kind of notable change in cytosolic Ca^{2+} concentrations is the reason behind enhanced GAD activity. Further, nuclear magnetic resonance has also been used to establish the three-dimensional structure of CaM bound to the petunia GAD CaM-binding domain (Yap et al., 2003) revealing an intriguing combination of CaM with two peptides of the CaM-binding domain. According to earlier research based on immunological detection of natural GAD complexes (~500 kDa) in transgenic plants expressing the full-length or truncated GAD missing the CaM-binding domain (Baum et al., 1996), this discovery implies a function for CaM in controlling the creation or stability of the GAD protein complex. There is evidence of the existence of a rice GAD isoform devoid of a CaM-binding domain (Akama et al., 2001). The use of transgenic plants ectopically expressing either GAD or a mutant GAD lacking the ability to bind CaM provided further evidence for the importance of CaM binding to GAD *in vivo* (Baum et al., 1996; Akama and Takaiwa, 2007).

Unlike bacterial or animal GADs, the majority of plant GADs have a calmodulin (CaM)-binding domain at the C-terminal amino acid residue. At neutral pH, Ca^{2+}-CaM stimulates GAD activity (Shelp et al., 2012). It is demonstrated that plant GADs were stimulated by the

complex Ca^{2+}/CaM, but not separately by Ca^{2+} or CaM. This complex is capable of inducing enzymes for biochemical and molecular events in plant cells (Zielinski, 1998).

1.4.2 GABA-T

Different sources of GABA-T are specific for GABA as an amino donor. GABA is converted to succinic semialdehyde (SSA) by recombinant GABA transaminase (GABA-T), which efficiently uses pyruvate and glyoxylate to produce alanine and glycine, respectively (Shelp et al., 2012; Koike et al., 2013; Shimajiri et al., 2013). The availability of pyruvate, which is generated during glycolysis and used in the synthesis of alanine, is thought to control the activity of plant GABA-T. Alternatively, the availability of glyoxylate, which is generated by several pathways and used by hydroxypyruvate reductases and glyoxylate reductases, influences GABA-T activity (Shelp et al., 2012; Zarei et al., 2017). *Arabidopsis* is known to have a single GABA-T, although several other species have multiple GABA-Ts with comparable substrate preferences. For example, rice has four GABA-Ts (Shimajiri et al., 2013).

1.4.3 SSADH

A recombinant NAD-dependent SSA dehydrogenase (SSADH), regulated by NADH and adenylates, oxidizes succinic semialdehyde to succinate (Shelp et al., 2012). After that, succinate contributes to the TCA cycle, which breaks down tricarboxylic acid. Thus, through this GABA shunt, the carbon skeleton of glutamate eventually enters the TCA cycle, and a reversible process occurs. This is a significant phenomenon since a variety of stressors can alter redox equilibrium. In tomatoes, a single SSADH has been identified (Akihiro et al., 2008). As they bypass two TCA cycle processes, these three reactions—from glutamate to GABA, SSA, and succinate collectively refer to this process as the GABA shunt. Moreover, Knockout mutants of SSADH in *Arabidopsis* exhibited sensitivity to light, heat, and UV-B stresses, leading to increased hydrogen peroxide levels and cell death (Bouche et al., 2003). This finding suggests that mitochondrial SSADH of the GABA shunt plays a crucial role in restricting the levels of reactive oxygen intermediates in plants.

1.5 Response of GABA under abiotic stresses

To date, multiple abiotic stresses have been reported to stimulate GABA accumulation in plants, such as salt, flooding, and drought. Though many materials are incorporated by plants into their bodies as a defense mechanism to withstand harsh environments. High amounts of GABA accumulate quickly in plant cells subjected to a range of stimuli, and there is strong evidence that GABA regulates tolerance against multiple abiotic stresses such as salt, drought, or extreme temperature (Kinnersley et al. 2000).

1.5.1 Salinity

Soil salinity and saline water inundation can cause considerable damage and yield loss in a wide range of crop plants. In poplar, saline conditions significantly enhance the expression levels of GABA and GAD mRNA (Ji et al., 2020). On the fourth day of salt treatment, it was demonstrated that exogenous GABA increased endogenous GABA, proline,

glutamate, alanine, glycine, lysine, threonine, and aspartic acid-like amino acids, as well as the GAD activity in *Solanum lycopersicum* leaves (Wu et al., 2020).

1.5.2 Water logging/ flooding

The submergence of land areas under water as a result of intense rainfall and the occurrence of tsunamis in coastal areas due to unpredictable changes in the climatic conditions cause the occurrence of floods. GABA promotes reactive oxygen species (ROS) detoxification in plants, which is accomplished by triggering antioxidative defense mechanisms (Li et al., 2021; Wu et al., 2021). Furthermore, by activating antioxidant enzymes, downregulating enzymes that produce reactive oxygen intermediates, and enhancing chloroplast function and photosynthetic characteristics, GABA enhanced the development of maize seedlings under waterlogged circumstances (Salah et al., 2019).

1.5.3 Drought

Drought is a xeric state caused by reduced water in the soil horizon as a result of factors such as reduced rainfall, low precipitation, and scarcity of water, among others. Reduced rates of photosynthesis, stomatal movement, and photosynthetic quantum efficiency are among the key characteristics of drought, along with elevated H_2O_2 and Malondialdehyde (MDA) levels and electrolyte leakage in plants (Riyazuddin et al., 2021). Amino acids and certain organic chemicals accumulate as a result of GABA enhancement under drought stress, which lowers oxidative damage by controlling the antioxidative system (Abdel et al., 2021; Hasan et al., 2021). Exogenous application of GABA raised endogenous GABA content and improved drought tolerance in white clover by upregulating the GABA shunt, polyamines, and proline metabolism (Yong et al., 2017).

1.6 Genome editing and CRISPR/Cas9 technology

A collection of cutting-edge molecular biology methods that enable accurate, effective, and targeted alterations at genomic loci is known as genome editing (Chen et al., 2013, Gao, 2015). Double strand break (DSB) is the first step in genome editing, and it is caused by a site-specific nuclease. Homologous recombination (HR) and non-homologous end joining (NHEJ) are the two basic methods for repairing damaged DNA ends (Liu et al., 2018). Two pathways namely, homology-directed repair (HDR) and non-homologous end joining (NHEJ) mechanisms—are used to repair the DSBs created by the Cas-9 protein (Liu et al., 2018). By introducing a donor DNA template with sequence homology at the anticipated DSB location, HDR carries out the targeted gene modification (Liu et al., 2018; Yang et al., 2020).

Utilizing the clustered regularly interspaced short palindromic repeats (CRISPRs)-Cas system, particularly CRISPR-Cas9, has greatly expanded genome editing in plants in recent years (Jinek et al., 2012). Targeted mutations have been introduced into plants using the CRISPR/associated nuclease Cas9 system to investigate gene function and open up new crop enhancement opportunities (Voytas et al., 2014; Gao, 2015). There are two main advantages of using a genome editing system: the first is the ability to introduce mutations at specific sites with accuracy and efficiency. Second, there is no discernible difference between the changed crops and those produced using traditional breeding methods (Nonaka et al., 2017;

Akama et al., 2020). Therefore, this quick and precise method is now being utilized to create gene knockout mutants, substitution mutation, or to insert gene fragments.

The RNA-guided CRISPR-Cas9 technique is one of the easiest genome editing methods to employ. It is predicated on how bacteria and archaea's adaptive immune systems allow them to react and get rid of invasive viruses and plasmids (Jinek et al., 2012; Cong et al., 2013). The Cas9 nuclease from *Streptococcus pyogenes* (or comparable substitutes), crRNA, and tracrRNA make up this system's three parts. Targeted double-stranded breaks in genomic DNA may now be introduced with a simpler two-component reagent that was created by combining the tracrRNA and crRNA into a single synthetic single guide RNA (sgRNA) (Miladinovic et al., 2021). With this approach, guide-RNA makes Watson–Crick base pairing with complementary genomic DNA strand, and Cas9 endonuclease makes double-strand DNA cleavage in the genome DNA at 3 bases upstream to PAM (protospacer adjacent motif) site. Through the utilization of native cell machinery, NHEJ or HR mediates the repair of the double stand break (DSB) produced by Cas9. Due to the error-prone nature of the NHEJ repair pathway, the double-strand break location may experience deletions or insertion mutations (Kumar et al., 2020). However, there are additional factors to take into account when assessing the possibility that genome editing would result in an off-target mutation. Compared to genetically modified crops, the hazards of using genome-editing technologies to modify genomes are far lower. In this instance, the majority of edits only modify a small number of nucleotides, resulting in modifications that resemble those observed in naturally occurring populations (Zhang et al., 2018)

1.7 Rationale for study with GAD4

Out of the five *OsGAD* genes, research has previously been done on *OsGAD1*, *OsGAD2*, and *OsGAD3*, and the findings of those studies were intriguing. Prior research on *OsGAD1* has reported its ability to bind to CaM. Additionally, *OsGAD2* mutants missing the C-terminal extension exhibited increased GABA levels but were unable to bind CaM (Akama et al. 2001; Akama et al., 2007). In rice grains, the deletion of the C-terminal coding region of *OsGAD3* increased GABA accumulation by seven-fold compared to wild type (Akama et al., 2020). The C-terminal region of *Os*GAD4 was assumed to bind Ca^{+2}/CaM to CaMBD (Yasuda, unpublished). Therefore, deletion of CaMBD may lead to a rise in GAD activity and truncated mutants with improved GABA production are the expected outcome. The expression level of *OsGAD4* is highest in germinated brown rice among the five *OsGAD* genes (Zhao et al., 2017). So, our hypothesis is truncation of the C-terminal region of *OsGAD4* may result in enhanced accumulation of GABA in not only brown rice but also other vegetative tissues. We chose *Os*GAD4 as the target gene for this investigation based on the above-stated hypothesis.

1.8 Aim of the study

The goal of the project is to truncate the Ca^{2+}/calmodulin-binding domain (CaMBD) of the C-terminal region of rice GADs to create GABA-fortified rice plants by genome editing of the rice GAD4 gene and further detailed analysis of the mutant under abiotic stress treatments.

Chapter II: Production of GABA-fortified rice through CRISPR/Cas9 genome editing

2.1 Introduction

Rice is the major diet for more than half of the world's population, notably in Asia (Fukagawa et al., 2019), where it provides an important source of carbs and minerals. However, despite its extensive use, rice frequently lacks bioactive chemicals that are helpful to human health. Providing nutritive ingredients from rice as a staple diet is critical for meeting global nutritional demands, guaranteeing food security, conserving cultural heritage, fostering economic growth, and encouraging environmental sustainability. Rice, when combined with other nutrient-enriched compounds, improves the overall health and well-being of individuals and communities across the world. Gamma-aminobutyric acid (GABA), a non-proteinogenic amino acid, has gained popularity in recent years due to its potential health benefits. It regulates neurotransmission, controls blood pressure, and reduces stress. Its presence in food goods has sparked widespread interest due to its possible health advantages. Previous research shows that GABAergic (chemical that modifies the effects of GABA in the body or brain) receptors modulate the intestinal innate immune response, which aids in immunological homeostasis (Zheng et al., 2021). Furthermore, GABA has been found to influence physiological activities such as maintaining blood pressure (Tanaka et al., 2009), and anti-aging (Huber et al., 2018) among others.

Traditional breeding approaches for increasing GABA concentration in rice have been constrained by genetic restrictions and time-consuming processes. In recent years, CRISPR/Cas9 genome editing technology has transformed crop development by providing accurate, rapid, and efficient tools for targeted genetic modification. This approach allows for the introduction of specific mutations, insertions, or deletions into the genome, which facilitates the alteration of genes involved in GABA production pathways in rice. Researchers have already boosted GABA accumulation in rice grains by targeting critical genes that regulate GABA metabolism, such as glutamate decarboxylase (GAD) (Akama et al., 2020). GABA-fortified rice produced via CRISPR/Cas9 genome editing has various benefits over standard breeding methods. First, CRISPR/Cas9 allows for precise and predictable gene modifications, reducing unexpected genetic changes and off-target consequences. Furthermore, the effectiveness and speed of CRISPR/Cas9-mediated genome editing enable the quick production and screening of modified rice lines with higher GABA content.

2.2 Materials and methods

2.2.1 Plant Materials and Growth Conditions

Rice cultivar namely, *Oryza sativa* L. cv. Nipponbare (Ni) was used for the transformation in this study. Rice seeds were surface sterilized in 75% (v/v) ethanol for 1 min with gentle shaking, followed by washing with double distilled water (ddH_2O). Then seeds

were transferred to 50% (v/v) commercial bleach solution (Haitar; Kao Co., Ltd., Tokyo, Japan) for 30 min with continuous shaking. After rinsing 5 times with ddH_2O, seeds were sown in 0.5 × Murashige and Skoog (MS) solid media (Murashige and Skoog, 1962). Then, the seeds were allowed to germinate in a 25°C growth chamber (SANYO, Osaka, Japan), with a 16 h light/8 h dark photoperiod. Later, the geminated rice seedlings were cultivated in a growth room with LED light (LCL-W5-1200, Churitsu Electric Corporation, Nagoya, Japan) at 25°C temperature with the same photoperiod mentioned above. The plants were transferred to a naturally lighted non-contained greenhouse (40 m^2 in area) located at Shimane University, Matsue, Japan, as reported by Akama et al. (2009).

2.2.2 Ca^{2+}/CaM-Binding Assay

In-vitro Ca^{2+}/CaM-Binding assay was performed following the methods stated in Akama et al. (2001). Recombinant protein with *Os*GAD4-CaMBD and *Os*GAD3-CaMBD fusion protein was used in this experiment.

2.2.3 Plasmid Construction

Genome-editing vectors were constructed for truncation of the C-terminal coding region of *OsGAD4*. The CRISPR-P program (Lei et al. 2014) was used for designing single guide RNA (gRNAs) for truncation of the C-terminal region of *Os*GAD4: guide RNA (gRNA) in the coding region for the *Os*GAD4-CaMBD targeted upstream (gRNA-F1) and downstream (gRNA-R1). A couple of the synthesized 20-nucleotide target sequences for gRNA-F1 and gRNA-R1 (Fig. 7a) were annealed to make double-stranded DNA, respectively, and then inserted into the *Bbs*I site of the gRNA cloning vector pU6gRNA (Mikami et al. 2015). A *Pvu*II and *Asc*I fragment from pU6gRNA carrying gRNA-R1was inserted into pU6gRNA carrying gRNA-F1 via the *Eco*RV and *Asc*I sites respectively, resulting in pU6gRNA_F1 and R1. A *Pvu*II and *Asc*I fragment from this pU6gRNA derivative was inserted at the *Asc*I and *Plm*I sites of a Ti plasmid pZH_gYSA_MMCas9 (Mikami et al. 2015) for rice transformation.

2.2.4 *Agrobacterium*-Mediated Rice Transformation

Rice transformation using *Agrobacterium tumefaciens* is a method of choice due to stable and low copy number integration of transfer-DNA (T-DNA) into the plant chromosome and transfer of larger DNA segments with defined ends. The binary vector was introduced into *Agrobacterium* strain EHA105 (Hood et al. 1993). *Agrobacterium* transformation of rice calli, selection of proliferating calli with N6D media supplemented with 50 mg/L of hygromycin B, and subsequent regeneration was done principally as described by Ozawa (2009).

2.2.5 List of media with composition

Table 1. Media used in this study

Name	Composition
0.5x MS (Murashidge and Skoog) media (Akama et al., 2009)	2.35 g/L of MS powder (Wako, Japan) was dissolved in de-ionized water, pH adjusted at 5.8 by NaOH or HCl using pH meter. Gelrite: 4 g/L was added and placed for autoclave at 121°C, 15 psi for 20 minutes.
Selection media N6 (Chu) media (Lei et al., 2014)	Sucrose (30 g/L), N6 basal salt (Sigma, Japan) (3.98 g/L), Myo-inositol (100 mg/L), Casamino acids (300 mg/L), Proline (1150 mg/L), pH adjusted at 5.8. Gelrite (4 g/L). After autoclave, the media was supplemented with 2,4 D (200 µl/L), PPM (plant preservative mixture) (500 µl/L), Vitamin (1 ml/L), Hygromycin (1 ml/L), Meropen (1 ml/L).
Regeneration media (Mikami et al., 2015)	MS powder (4.70 g/L), Sucrose (30.0 g/L), Sorbitol (30.0 g/L), Casamino acid (2.0 g/L), pH adjusted at 5.8 by NaOH or HCl. Gelrite (4.0 g/L) was added. After autoclave the media was supplemented with NAA (α-naphthaleneacetic acid) (0.2 mg/L), Kinetin (2.0 mg/L), Meropen (1 ml/L), Hygromycin (1 ml/L), PPM (500 µl/L)
Hormone free media	MS powder (2.35 g/L), adjust pH at 5.8. Gelrite (4 g/L), After autoclave the media was supplemented with PPM (500 µl/L) and Hygromycin (500 µl/L)

MS media was commonly used for growing seedlings in Petri dishes and subsequently in glass tubes. Moreover, selection media, regeneration media, and hormone-free media were used in the rice transformation process.

2.2.6 DNA lysate preparation and PCR for screening

DNA lysates were prepared using the leaves of young seedlings for screening of transgenic lines. A small section (2-3 mm^2) of the leaf was taken and placed in a 96-well PCR plate containing 50 µl of elution buffer (1 M KCl, 100 mM Tris-HCl [pH: 8.0], 10 mM EDTA) in each well. Then, it was heat boiled for 5 minutes at 95°C. PCR master mix, KAPA (KAPA BIOSYSTEMS, United States) was used for amplification from the DNA lysate for screening purposes along with forward and reverse primers of the target region. PCR conditions were hot start at 95°C for 3 min and then 38 cycles of denaturation at 95°C for 15 s, annealing at 60°C for 15 s, and extension at 72°C for 20 s. An automated microchip electrophoresis system MultiNA (Shimadzu Co. Ltd., Kyoto, Japan) was used to analyze the PCR products. Moreover, to screen out the transgenic plants, rice leaves were collected from the plants grown in the greenhouse to extract genomic DNA using the cetyltrimethylammonium bromide (CTAB) method (Murray and Thompson 1980). For doing PCR analysis of the genomic DNA samples, 10× *Taq* buffer (100 mM Tris-HCl: pH 9.0 at 25°C, 500 mM KCl,

and 15 mM $MgCl_2$ and 1% Triton X-100), *Taq* DNA polymerase (Takara), dNTP, and forward and reverse primers (F1 and R-356 respectively) were used.

2.2.7 Genomic DNA isolation

Genomic DNA was isolated from Nipponbare and genome-edited rice leaves in the vegetative stage. The plant material, ~50 mg fresh leaves from each of the plants, was frozen on liquid nitrogen and crushed in screw cap tubes (2 ml) containing small (5 mm) stainless steel beads (Microsmash TOMY, Tokyo, Japan). Genomic DNA was isolated using the CTAB (Cetyl trimethylammonium bromide) method:
At first, 2% CTAB buffer (Table 3) was mixed with 0.2% (v/v) 2-mercaptoethanol in a 2 ml tube and 400 µl of CTAB buffer was added to the plant material, shaken gently, and homogenized the samples. Then placed in heat-block incubator (60ºC) for 30 minutes, shaken occasionally. 400 µl of Chloroform: Isoamyl alcohol (24:1) mixture was added and mixed well. Centrifuged at 14000 x *g* for 10 minutes at 4ºC to transfer the aqueous phase to a new 1.5 ml clean microcentrifuge tube. After that, 200 µl cold isopropanol was added for DNA precipitation and mixed well. Centrifuged at 14000 x *g* for 10 minutes at 4ºC and supernatant was discarded keeping the pellet. Then air dried the DNA pellet, was dissolved in 100 µl TE (10µg/ml RNaseA), mixed well by vortex (IWAKI), and incubated for 30 minutes at 30ºC.

Afterward, 100µl TE (10mM Tris-1mM EDTA) buffer (pH 8), 100µl 7.5M Ammonium Acetate (pH 5.5), 750 µl 100 % Ethanol was added, mixed well, and vortex for 5 min. Again centrifuged at 14000 x *g* for 20 minutes at 4ºC and the supernatant was discarded keeping the pellet. After ethanol precipitation, the DNA pellet was allowed to dry and dissolved in 100µl TE and thus the concentration of DNA was confirmed by electrophoresis of the individual samples on 1% agarose gel. After that genomic DNA was used for PCR reaction.

2.2.8 List of primers

Table 2. Primers used in this study

Name	Sequence (5' to 3')	Experiment
gRNAF1-F	GTTGGCCCGCGTCGTCGCCAACGG	**Genome editing**
gRNAF1-R	AAACCCGTTGGCGACGACGCGGGC	
gRNAR1-F	GTTGGGATGAGAGCAGACTTGAGA	
gRNAR1-R	AAACTCTCAAGTCTGCTCTCATCC	
GAD4- F1	CATCCGCGAGGACTTCAG	**Analysis of genome edited plants**
GAD4- R356	AGCAGCATCAATCCGAAAAT	
GAD4-F	ACCGTCTCAAGTCTGCTCTCAT	**RT-qPCR**
GAD4-R	TCAATTCACTGCTACACACCCA	
TBP2-F	TGGTCTGGAGGAGCGTATAGCA	**Internal control in RT-qPCR**
TBP2-R	CAAGTCTCTCAGTCACCCAAGC	

2.2.9 List of buffers with composition

Table 3. Buffer used in this study

Name	Composition
Elution buffer	Used for DNA lysate preparation 1 M KCl, 100 mM Tris-HCl (pH: 8.0), 10 mM EDTA
CTAB (Cetyltrimethylammonium bromide) buffer	Used for genomic DNA isolation from fresh tissue of rice plants. 1.4 M NaCl, 20 mM EDTA, 100 mM Tris-HCl, CTAB The buffer was supplemented with 0.2% of 2-meraceptoethanol during use.

2.2.10 DNA Sequencing

PCR of genomic DNA with Emerald:

Emerald is a Master Mix (TAKARA Bio) ensures PCR specificity and includes an optimized buffer, PCR enzyme, dNTP mixture, gel loading dye (green) and a density reagent in a convenient 2X premix format.

Template – 0.5 µl

Emerald master mix - 5µl

Primer F1 - 0.4 µl

Primer R 356 – 0.4 µl

dMQ – to adjust the volume upto 10 µl.

PCR condition

95ºC for 1 min

Denaturation (98ºC, 10 S),

Annealing (55ºC, 30 S),

Extension (72ºC, 30 S) and 30 cycle

Then the PCR product was checked with gel electrophoresis. When clearly visible single band was found, it was used for further reaction.

Enzyme treatment for PCR Product clean-up

This step is done to clean up the PCR product through single-step purification. It removes unreacted primers and dNTPs in one step. ExoSAP-IT (Thermo Fisher Scientific) purified samples can be used in downstream applications such as DNA sequencing.

PCR product- 6 µl

dMQ- 14 µl, mix well to volume 20 µl.

EXO SAP IT - 1µl, diluted in 40 µl of dMQ and added 4 µl in each sample.

Incubated at 37ºC for 60 min

And 80ºC for 15min

Sequence reaction (Big Dye terminator Kit, Applied Biosystems, USA)

Template -1 µl

5X IB -1.9 µl
Brilliant dye terminator -0.2 µl
Primer (F1 or R356) -0.3 µl
dMQ - to adjust the volume up to 10 µl
Reaction condition:
95ºC for 5 min
Denaturation (95ºC, 30 S),
Annealing (52ºC, 10 S),
Extension (60ºC, 4 min) and 30 cycle

Ethanol precipitation

- 1µl of 3M sodium acetate (pH: 5.2) and 25 µl of 100% ethanol were added to the DNA template in a 1.5 ml microtube. Mixed well by pipetting.
- Kept in rest for 15 minutes at room temperature in dark place.
- Centrifuged at 14,000 x *g* for 20 min at 4ºC.
- The supernatant was discarded.
- 20 µl of 70% ethanol was added
- Again, centrifuged at 14,000 x *g* for 10 min at 4ºC.
- The supernatant was discarded.
- The sample was dried in a dark place.
- 15 µl of Hi-Di formamide was added to each sample and vortexed to mix it well.
- Denaturation was done at 95ºC, for 5 minutes and immediately cooled on ice.
- Then the sample was placed on ABI PRISM 3130 xl Genetic Analyzer (Applied Biosystems).

The DNA sequences found after this experimental process were read using GENETYX-MAC Software v.22.0.1 (GENETYX Corporation).

2.2.11 Amino acid isolation

- The plant material (leaf, stem, and grain), ~50 mg from each plant, was frozen on liquid nitrogen (in the case of vegetative tissues) and crushed in 2 ml screw-cap tubes containing small (5 mm) stainless steel beads.
- 40 mg plant material was measured and transferred to a 1.5 ml microtube.
- Added 400 µl of 8% TCA (Trichloro acetic acid) (volume is 10 times of the material)
- Shook for 30 min (IWAKI TUPLE MIXER, Japan)
- Centrifuged for 20 min at 14,000 x *g* at 20ºC
- Transferred the aqueous clear solution to a new tube
- Added Di-ethyl ether at least twice the volume of the solution in the tube
- Shook for 30 min
- Centrifuged for 20 min at 14,000 x *g* at 20ºC
- Repeated the process from the addition of Di-ethyl ether
- Dry the solution of amino acid to remove the extra Di-ethyl ether.

2.2.12 GABase (sigma) Assay:

It is the enzymatic assay used to determine GABA concentration in plant tissues. GABase is a commercially available mixture of γ-aminobutyric acid Transaminase (GABA-T) and succinate semialdehyde dehydrogenase (SSDH) from *Pseudomonas fluorescens* (Sigma). GABase from *Pseudomonas fluorescence* is used in the GABase assay to quantify the concentrations of GABA (γ-aminobutyric acid).

Twelve GABA standards were prepared to compare the GABA content having the concentration of 0 nmol/20 µl, 0.1 nmol/20 µl, 0.25 nmol/20 µl, 0.5 nmol/20 µl, 1.0 nmol/20 µl, 1.5 nmol/20 µl, 2.0 nmol/20 µl, 2.5 nmol/20 µl, 3.0 nmol/20 µl, 5.0 nmol/20 µl, 10 nmol/20 µl and 20 nmol/20 µl.

A reaction mix (volume is 150 µl) was prepared including the following materials

0.1 M Pyrophosphate buffer (pH 10.5)	-142 µl
60 mM 2-mercaptoethanol	-4 µl
60 mM α-Ketoglutarate	-2 µl
50 mM NADP+	-2 µl
Total	=150 µl

NADP =Nicotinamide Adenine Dinucleotide Phosphate

20 µl of the amino acid sample was taken in a 96-well special plate for GABase analysis. Then 150 µl of reaction mix was added to each sample. The plate was set in a Fluorescence photometer (TECAN, Wako Genios FL, Austria) and zero adjustment was done for standard and unknown samples.

GABase mix (volume is 10 µl per sample) was prepared as follows:

GABase – 2 µl/per reaction

0.1 M Pyrophosphate buffer – 8 µl

Mixed well and placed in an incubator (37ºC for 60 min)

Then again placed in the photometer machine to measure the GABA content of the unknown samples. To measure the content of GABA, the absorbance was measured after and before incubation, and the differences were calculated.

The value found from the unknown sample is in the unit of 1.0 nmol/2 mg. So, we convert the value to 0.5 nmol/mg FW (Fresh weight) or, 0.5 µmol/g FW.

2.2.13 Gas Chromatography/ Mass Spectrometry

The concentration of each free amino acid was determined by gas chromatography/mass spectrometry (GC/MS) as follows: samples were derivatized using the dedicated EZ:Faast™ kit (Phenomenex, Torrance, CA), followed by analysis using a GC/MS-QP2010 system (Shimadzu Co. Ltd., Kyoto, Japan) with electronic pressure control and equipped with a split capillary inlet. A 1-µl aliquot of each sample was injected in split mode into the system [injection temperature 280°C; ZB-AAA column (length 10 m, diameter 0.25 mm; Phenomenex); helium gas flow rate 3.0 ml/min].

Standards

Three vials of different standard mixtures are included in the kit:

SD1: 23 amino acids, 200 nmol/ml each as follows: α–Aminoadipic acid, Aspartic Acid, Glycine, Leucine, Phenylalanine, Threonine, α-Aminobutyric acid, β –Aminoisobutyric acid, Histidine, Lysine, Proline, Tyrosine, Isoleucine, Cystine, Hydroxyproline, Methionine, Sarcosine, Valine, Alanine, Glutamic acid, also-Isoleucine, Ornithine, Serine
SD2: Complementary amino acids not stable in acidic solution, 200 nmol/ml each as follows: Asparagine, Glutamine, Tryptophan
SD3: Complementary urine amino acids, 200 nmol/ml each as follows: α–Aminopimelic acid, Cystathionine, Glycyl-proline, Hydroxylysine, Proline-hydroxyproline, Thioproline

GABA standard

GABA standards were prepared manually for our use in the GC/MS experiment.
Six standards: 1 nmol/ml, 5 nmol/ml, 10 nmol/ml, 50 nmol/ml, 100 nmol/ml and 200 nmol/ml.
Calibration Solution:

I. 25 µl of SD solution, plus 100µl Reagent 1(calibration level I: 50 nmol/ml)
II. 50 µl SD solution, plus 100µl Reagent 1(calibration level II: 100 nmol/ml)
III. 100 µl SD solution, plus 100µl Reagent 1(calibration level III: 200 nmol/ml).

Internal standard

The use of an internal standard best compensates for the variability generated in sample hydrolysis and amino acid analysis. Norvaline is the standard used as an internal standard. The concentration of the internal standard in the sample prepared for gas-chromatographic analysis is 200 nmol/ml.

Calculation of results

Calculations were performed by the data analysis portion of the software controlling the analytical instrument. Calculations and calibration were based on the internal standard.

2.3 Results

2.3.1 The C-terminal region of *Os*GAD4 can bind to Ca^{2+}/CaM

We compared eight amino acid sequences in the C-terminal regions of GADs from 3 plant species (Fig. 3a). The C-terminal region of almost all plant GADs has s Ca^{2+}/CaMBD, which was first reported in *Petunia hybrida* GAD (*Ph*GAD) to regulate the GABA biosynthesis in plants (Baum et al. 1993). On the contrary, it has also been discovered that the rice GAD2 isoform (Fig. 3a) lacks a CaMBD (Akama et al. 2001). Plant GADs exhibit little similarity in their C-terminal extensions, as illustrated in Fig. 3a; nevertheless, they do share certain features, such as the presence of multiple conserved clusters in each GAD. In particular, the domain's centre contains a highly conserved tryptophan (W) residue. Moreover, the N- and C-termini of GAD exhibit 2 to 4 arginine (R) and lysine (K) clusters. Important roles in the binding of CaM to the CaMBD are played by the lysine (K) clusters and the tryptophan (W) residue (Arazi et al. 1995). According to a report by Yap et al. 2003, E476 and E480 work as pseudosubstrates of glutamic acid (Glu) in *Petunia* GAD and have autoinhibitory functions in the absence of Ca^{2+}/CaM binding. Results such as these leave us in no doubt that the Glu residues are conserved in all the C-termini of rice isoforms, excluding *Os*GAD2, indicating a probable conserved function. Between two tea GADs (*Cs*GAD), *Cs*GAD2 cannot bind to CaM but it is upregulated by mechanical stress, whereas *Cs*GAD1 can bind to CaM (Mei et al. 2016). According to the sequence alignment, *Cs*GAD1 has the conserved motifs at the C-terminus, while *Cs*GAD2 lacks one Lys (K487) and one Glu (E471) residue. Previous studies reported the *in vitro* Ca^{2+}/CaM binding abilities of *Ph*GAD, *Os*GAD1, and *Os*GAD3 (Baum et al. 1993; Akama et al. 2001; Akama et al. 2020), thus we anticipated that *Os*GAD4 potentially has the same ability, because it contains all the characters that are required for binding to Ca^{2+}/CaM. It was speculated from the structural features of *Os*GAD4-CaMBD that *Os*GAD4 is a common plant GAD that demonstrates Ca^{2+}/CaM-dependent activation (Fig. 3a). In α-helical wheel analysis, all of the hydrophobic residues are grouped on one side of *Ph*GAD, whereas residues with positive charges are on the opposite side (Fig. 3b). The Trp (W) residue and Lys (K) cluster, which assist hydrophobic and electrostatic interactions, respectively, are critical for efficient CaM binding to the CaMBD of *Ph*GAD (Arazi et al. 1995). *Os*GAD4 and *Ph*GAD were identical at these crucial points, while *Os*GAD2 had a different structure. Additionally, *Cs*GAD2 exhibited differences in two conserved motifs within the essential domain. The analysis of the α-helix in Figure 3b validates the hypothesis that *Os*GAD4 can bind Ca^{2+}/CaM at the CaMBD.

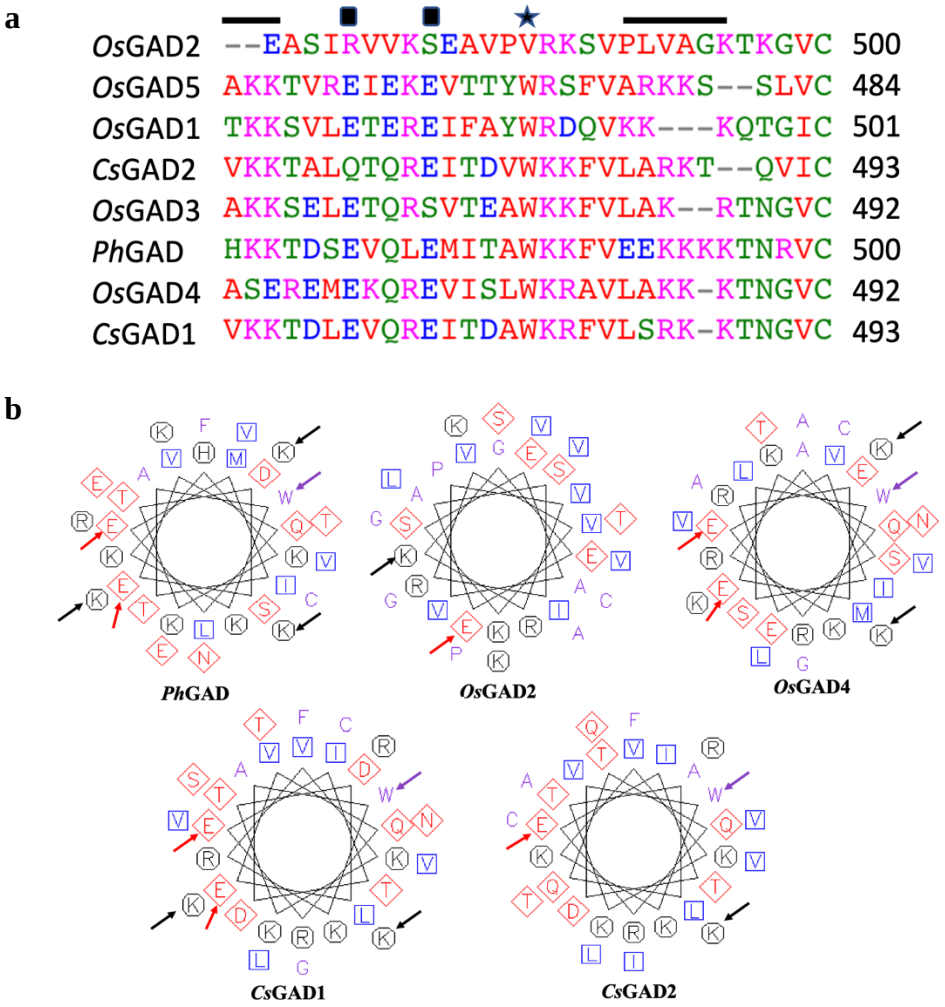

Figure 3. Comparison of the C-terminal regions of plant GADs.

a) Multiple sequence alignment of the C-terminal regions of GADs in rice, petunia, and tea. Trp (W) and Lys (K) essential for *in vitro* binding to CaM are indicated by stars and a thick line, respectively. The positions of two pseudosubstrate residues E476 and 480 in *Ph*GAD are indicated by rectangles, reported by Arazi et al. (1995). *Os*: *Oryza sativa*, *Ph*: *Petunia hybrida*, *Cs*: *Camellia sinensis*. *Os*GAD1 (AB056060), *Os*GAD2 (AB056061), *Os*GAD3 (AK071556), *Os*GAD4 (AK101171), *Os*GAD5 (AK070858), *Ph*GAD (L16977), *Cs*GAD1 (KT728367), *Cs*GAD2 (KT728368). **b)** α-Helical wheel projection of amino acid residues displayed using EMBOSS-pepwheel (https://www.bioinformatics.nl/cgi-bin/emboss/pepwheel). Hydrophobic residues are marked with squares, hydrophilic residues with diamonds, and positively charged residues with octagons. The hydrophilic area is clustered on the opposite side of the Trp (W)-centered hydrophobic residues (purple arrows). W and the Lys (K) cluster (black arrows) at the C-terminus are essential for the effective binding of CaM to the GAD-CaMBD. They contribute to hydrophobic and electrostatic interactions. The red arrowed Glu (E) residues serve as pseudosubstrates.

2.3.2 *In vitro* CaM-binding assay confirms that Ca^{2+}/CaM -Binding Domain of *Os*GAD4 is capable of CaM Binding

To verify if the C-terminal domain of *Os*GAD4 is capable of Ca^{2+}/CaM -binding, an expression vector carrying a DNA fragment for the C-terminal domain of *OsGAD4* was constructed to over-express in *E. coli* strain BL21 (DE3) pLysS and to purify recombinant protein it was incubated with bovine CaM agarose beads in the presence of Ca^{2+}. As a result of binding with Ca^{2+}/CaM, it will be expected that the C-terminal region of GAD4 is eluted with EGTA-containing buffer, whereas the control protein expressed from only vector is detected on the reverse side. The recombinant protein with the C-terminal region of *Os*GAD4 was not detected in the effluent fractions (Lanes: 2 to 5) (Fig. 4) but was detected in the elution fractions (Lanes: 6 to 8; corresponds to the recovery of first, second, and third elution with elution buffer with EGTA, respectively). Conversely, the vector control's elution fractions showed no signs of protein. Moreover, for further confirmation of the result of this experiment, another expression vector carrying a DNA fragment for the C-terminal domain of *Os*GAD3 was used as a positive control (Akama et al. 2020).

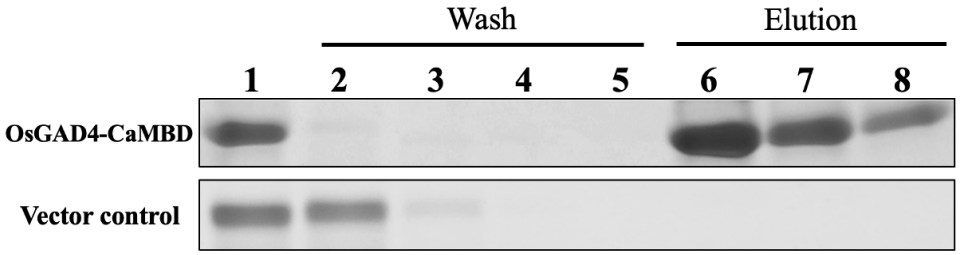

Figure 4. *In vitro* CaM-binding assay with recombinant *Os*GAD4-CaMBD fusion protein and vector control.

An expression vector carrying a DNA fragment for the C- terminal domain of *Os*GAD4 was constructed. Coding sequence for the C-terminal peptide of *Os*GAD4 cDNA was subcloned in-frame in pET32a (Novagen) and transformed into *E. coli* strain BL21 (DE3) pLysS. Recombinant protein carrying a polyhistidine-tag was induced for purification using a nickel-affinity resin. Expression of the fusion protein (*Os*GAD4-CaMBD), its purification and an *in vitro* CaM binding assay were performed in accordance with Akama et al. (2001). As a negative control, an empty expression vector (pET32a) was used. The protein was purified to incubate with bovine CaM agarose (Sigma) in the presence of Ca^{2+}, then the agarose beads were washed with an excess amount of Ca^{2+}-containing buffer four times. CaM-binding proteins were eluted with elution buffer containing EGTA three times. Protein samples were electrophoresed on a 15% SDS-polyacrylamide gel, followed by Coomassie Brilliant Blue staining. Lane 1: fusion protein in case of OsGAD4-CaMBD panel and vector encoding protein in case of vector control panel, Lanes 2-5: effluent fractions, Lanes 6-8: eluted fractions with EGTA-containing buffer.

2.3.3 *In vivo* truncation of the C-terminal region of *Os*GAD4-CaMBD by genome editing

OsGAD4 gene structure including exon/intron positions is demonstrated in Figure 5a, where the CaMBD is presumed to be in the proximal region of the last exon of the gene.

a

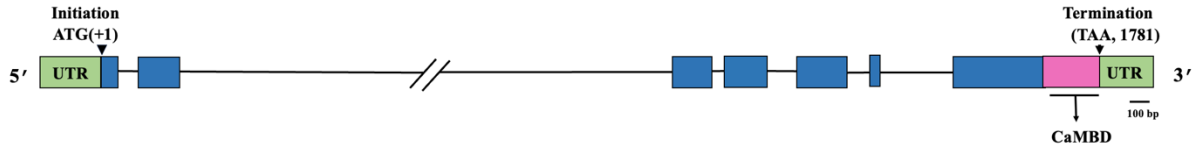

b

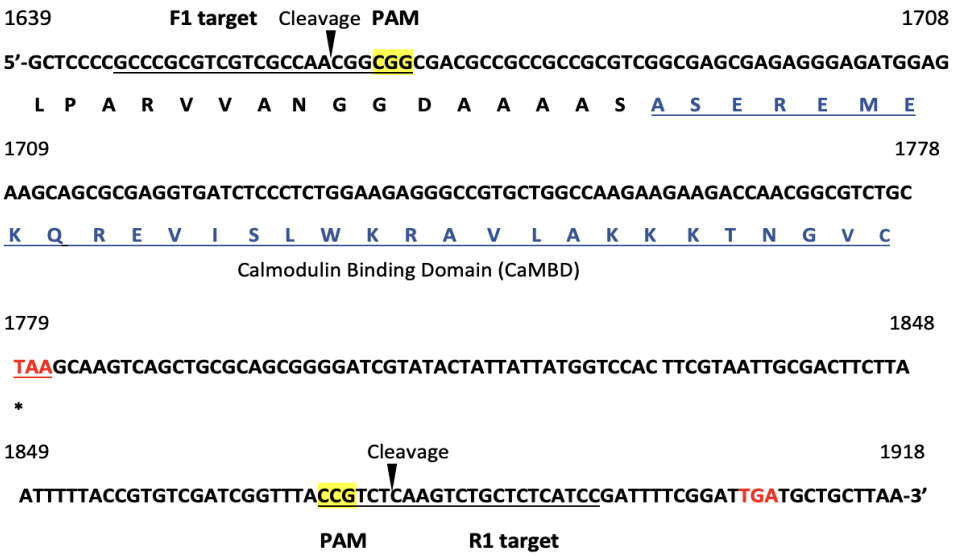

Figure 5. Schematic diagram of *OsGAD4* (ID: Os03g51080.1) gene structure and gRNA target site for genome editing

a. Schematic diagram of *OsGAD4* (ID: **Os03g51080.1**) gene structure.

Exons and introns are indicated by blue boxes and lines respectively. UTR indicates untranslated region shown as a green box; Double slash between the first intron indicates the sequence gap in the longest intron of this gene. Upstream and downstream arrows direct the translation initiation and termination sites, respectively. The number in brackets denotes the distance of the exon sequence to the initiation codon (ATG). Scale bar = 100 bp. **b**. Downstream region of OsGAD4 including the target site of CaMBD. Nucleotide position is indicated for 1639 to 1918. Amino acids are shown below the nucleotide sequence. Upstream and downstream guide RNA consisting of a 20-nucleotide long sequence is denoted by F1 and R1 respectively. Black arrows show the targeted cleavage site in gRNA. An asterisk indicates a termination codon. The protospacer adjacent motif (PAM) sequence is highlighted in yellow, and amino acid sequences underlined in blue specify the CaMBD. Two termination codons are shown in red letters. The first one is an authentic termination codon and the latter one is used after cleavage at the two cleavage sites and joining.

Fig. 5b illustrates the construction of guide RNAs (gRNAs) intended to eliminate the C-terminal extension of *Os*GAD4-CaMBD. It was predicted that the upstream and downstream cleavage of F1 and R1 would result in a 216 bp deletion (Fig. 5b). Following DNA repair caused the deletion of almost the entire CaMBD and resulted in the production of GAD4 protein without the C-terminal domain.

2.3.4 *Agrobacterium*-mediated plant transformation and screening after regeneration

Agrobacterium was used to transform calli produced from rice scutellum. The Cas9 gene cassette and gRNAs were inserted into the *Agrobacterium* strain using a binary vector. A total of 27 distinct transgenic lines (T0) were produced as a result of the regeneration procedure.

Ten lines were selected as candidate lines after genome editing those having shorter bands at around 180 bp along with the wild-type band at 400 bp simultaneously (Fig 6a). DNA sequencing of the two alleles (Allele 1: 400 bp and Allele 2: 180 bp) in three independent T_0 lines (#11, #14, and #26) was performed to know the exact mutation of the target site. Allele 1 contained two lines (#14 and #26) that shared the same sequence as the wild type and one line (#11) that had several substitutions that resulted in a little alteration to the amino acid chain. Conversely, allele 2 displayed a 216 bp deletion throughout all three lines, suggesting that full CaMBD was effectively truncated (Fig 6a). To confirm the desired mutations in the segregating generation, seeds from all T_0 lines were cultivated. Following harvesting, seeds were cultivated to examine targeted genome editing and determine the amount of GABA present.

a **b**

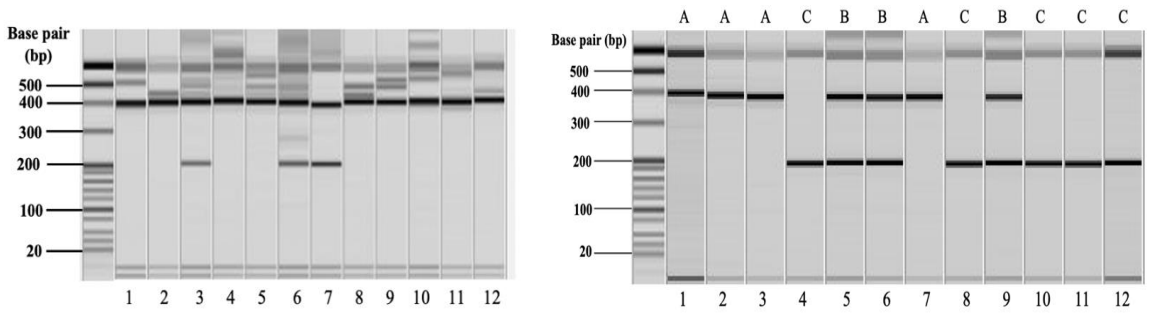

Figure 6. PCR screening of candidates of genome editing

a. Screening of regenerated candidates (T_0) through PCR and electrophoresis analysis by MultiNA (Shimadzu, Kyoto, Japan). We selected ten lines (three lines are shown) producing shorter band (along with the 400 bp band), B-type; as numbers 3, 6 and 7 in this figure. The rest are A-type lines producing only one band of 400 bp. **b.** PCR screening of transgenic plantlets (T_1 generation) with MultiNA (Shimadzu, Kyoto, Japan). DNA lysates were prepared by a boiling method, using young leaves of seedling; then this lysate was used as a template for PCR. A DNA size marker (20 bp to 500 bp) was used to identify the PCR product size. Here, A represents the mutant type similar to the wild-type (band size is 400 bp), B represents the heterozygous mutant (bi-allelic band), and C indicates the homozygous mutant (a band with an expected truncated size of around 180 bp) i.e., genome-edited bands. Twelve seedlings derived from the seeds of individual panicle were analyzed by PCR. Seedling numbers 1, 2, 3, and 7 were found to be similar to wild-type (A type); numbers 5, 6, and 9 were bi-allelic (B type), and the rest had the expected band size for genome-edited lines (C type).

Each T_0 line's seedlings were taken into consideration for PCR screening. For instance, twelve seedlings (T_1) germinated from a single panicle (#14 is shown in Fig. 6b) were analyzed by PCR. Three distinct patterns of amplified bands were revealed by PCR analysis of DNA isolated from the potential transgenic lines (T_1 generation) (Fig. 6b). The first pattern

(A-type) had a band at around 400 bp, which is similar to Nipponbare wild-type; the second pattern (B -type) had two bands at about 400 bp and 180 bp; and the third pattern (C-type) had only one band at about 180 bp. The last one was the anticipated amplicon size for the genome-edited lines, resulting from the 216 bp deletion. Out of the three distinct band patterns, A denotes mutants that are comparable to wild-type GAD4 mutants, B denotes the heterozygous state (bi-allelic), and C denotes the predicted homozygous mutant, or mutants that have undergone genome editing (Fig. 6b). Seedling numbers 1, 2, 3, and 7 were found to be A type; number 5, 6, and 9 were heterozygous B type, and numbers 4, 8, 10, 11, and 12 had the expected band size for homozygous genome-edited lines, C type. We eventually obtained 259 T_1 transgenic plants overall following a series of transformation events. Table 4a shows that 75 plants were identified as A type (29%), 114 as B type (44%), and 70 as C type. Differentiated genotyping results revealed a varied segregation pattern in the T_1 generation (Table 4b).

a

Total number of transgenic lines	Type of transgenic lines	Number of individual plants	Percentage (%)
T_0 (27)	A type	170	94.4
	Bi-allelic (B) type	10	5.6
T_1 (10)	A type	~75	~29
	Bi-allelic (B) type	~114	~44
	C type (expected band size)	~70	~27

b

	T_0 lines	#1	#11	#12	#14	#15	#19	#20	#24	#26	#27	Total
T_1	A type	8	6	7	8	7	6	11	5	9	8	~75
	B type	11	14	10	12	10	11	9	11	12	14	~114
	C type	9	9	6	8	4	8	8	5	6	7	~70

Table 4. Number of transgenic plants produced (T_0 & T_1) and their allelic states.
a. Quantitative data on produced mutants in T_0 & T_1 generation. We used the symbol ~, because during electrophoresis, some samples produced unclear bands, and few produced no band. So, this value is approximately or roughly counted. **b.** Separated genotyping data of transgenic lines producing A, B, and C type bands.

We have sequenced the T_1 generation's DNA and compared it to a Ni reference to validate the genome editing. The reference nucleotide is represented by wild-type Ni in Figure 7a; sequence analysis showed several types of genome-edited patterns, which are numbered 1 to 6. For DNA sequencing, the progeny of the #11, #14, and #26 lines were used. In this case, sequence number 1 (Fig. 7a) corresponds to type C (line #14), while sequence number 2 (line #14) corresponds to the slower migrating band in type B.

a

Ni reference F1 R1

5' – CGTCGTCGCCAACGGCGGCGACGCCGCCGCCGCGTCGGCGAG // GGCGTCTGCTAA //GTCTCAAGTCTGCTCTCATCCGATTTTCGGATTGA-3'

V V A N G G D A A A A S A S // G V C *

b

Genome Edited (GE)

1. CGTCGTCGCCAA - (-216 bp) - CAAGTCTGCTCTCATCCGATTTTCGGATTGA
2. CGTCGTCGCCAAa CGGCGGCGACGCCGCCGCCGCGTCGGCGAG//GGCGTCTGCTAA//TCT- - (-7 bp)- - -GCTCTCATCCGATTTTCGGATTGA
3. CGTCGTCGCCAAa CGGCGGCGACGCCGCCGCCGCGTCGGCGAG//GGCGTCTGCTAA//GTCTg CAAGTCTGCTCTCATCCGATTTTCGGATTGA
4. CGTCGTCGCCAACGGCGGCGACGCCGCCGCCGCGTCGGCGAG//GGCGTCTGCTAA// - - - (-27 bp) - - -CTCAAGTCTGCTCTCATCCGATTTTCGGATTGA
5. CGTCGTCGCCAAa CGGCGGCGACGCCGCCGCCGCGTCGGCGAG//GGCGTCTGCTAA//GTCTc CAAGTCTGCTCTCATCCGATTTTCGGATTGA
6. - - - - (-14 bp) - - - - GCTGGAGATG - - - (-8 bp) - - GAGAAGCAGCGCGAG//GGCGTCTGCTAA//GTCTCAAGTCTGCTCTCATCCGATTTTCGGATTGA

c

Amino acid sequence

Ni: VVANGGDAAAASASEREMEKQREVISLWKRAVLAKKKTNGVC

GE 1: VVANKSALIRFSD

GE 2: VVAKRRRRRRRVGERE.....FSD (80 AA)

GE 3: VVAKRGQPPRRVGKRK.....FIS (98 AA)

GE 4: VVANGGDAAAASASEREMEKQREVISLWKRAVLAKKKTNGVC

GE 5: VVAKRRRPPRRVGERE.....FIS (98 AA)

GE 6: WRWRSSARGRWRSSA.....ATS (53 AA)

d

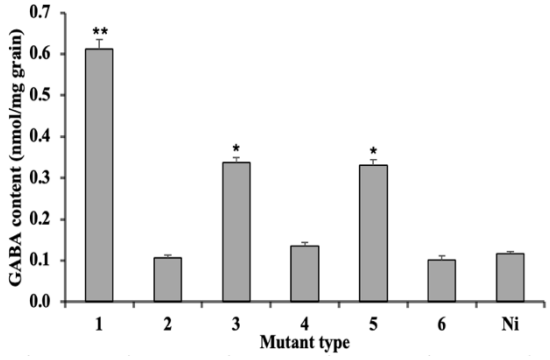

e

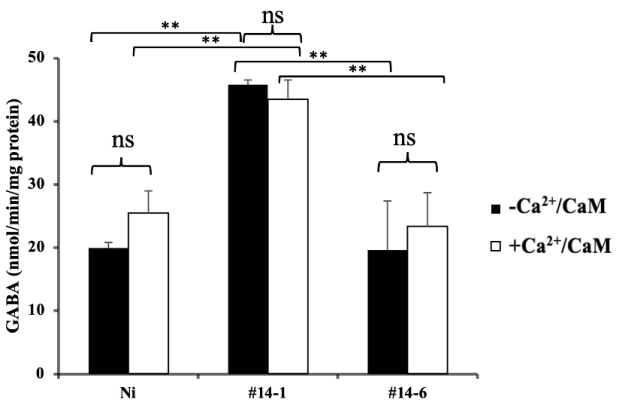

Figure. 7 Production of genome-edited plant and analysis

a) Nucleotide and amino acid sequences of *OsGAD4* transgenic plants; Wild-type Nipponbare (Ni) denotes the reference nucleotide sequence. The intended CRISPR/Cas9 cleavage sites are indicated by two black arrows (F1 and R1). The underlined text indicates the amino acid sequence from the CaMBD. Nucleotide sequence gaps and amino acid gaps are indicated by double slash marks. **b)** Nucleotide sequence of genome-edited lines numbers 1 to 6. In the genome-edited sequence, hyphens indicate the deletion; base pairs in parentheses indicate the length of the deletion. Small letters inside the box indicate insertions. **c)** Amino acid sequences of wild-type Ni and genome-edited lines (GE 1 to GE 6) resulted from the insertion and/or deletion of nucleotide sequences in the target region of CRISPR/Cas9, shown in Fig. 3c. The dots denote the amino acid sequence not shown in the polypeptide chain. The nucleotide sequence numbers 1 to 6 shown in Fig. 3c correspond to translated polypeptide chains GE 1 to GE 6 in Fig. 3d, respectively. In parentheses, the number along with AA indicates the length of the amino acid chain. DNA sequences were analyzed with GENETYX-MAC Software v.22.0.1 (GENETYX Corporation). **d)** GABA content in grains of C (sequence number 1), B (sequence number 2) and A type (sequence number 3 to 6) mutant. The concentration of GABA was measured by GABase assay. Error bars indicate SD (n=3). **e)** *In vitro* GAD enzymatic assay of total proteins extracted from the germ of Ni, #14-1 and #14-6 grains. This assay was performed to measure GABA production, following Akama and Takaiwa (2007) at physiological pH (pH 7). $-Ca^{2+}$/CaM; without Ca^{2+}/CaM, + Ca^{2+}/CaM; with 0.5 mM Ca^{2+} and 0.1 μM bovine calmodulin (Sigma). Error bars indicate SD (n=3). Two-way Analysis of variance (ANOVA) was used to determine the differences among various treatments. Asterisks indicate significant differences versus Ni (*$P < 0.05$, **$P < 0.01$). ns=not significant (no difference within groups).

The rest of the sequences, having different patterns, are all A type (lines of #11, #14, and #26). We found that the target region of CRISPR/Cas9 differed in amino acid sequence between genome-edited lines and wild-type Ni lines. The translated polypeptide chains, GE 1 to GE 6 in Fig. 7c correspond to nucleotide sequences from 1 to 6 displayed in Fig. 7b. After the authentic N-terminal VVAN, a peptide containing nine synthetic amino acids was produced by the deletion of the CaMBD. Longer polypeptide chains were a feature of the other alterations. GABA content was then ascertained from the grain following the acquisition of distinct sequence patterns in the B, C, and A type plants (T1 generation). When compared to wild-type Ni, a variety of GABA concentration values were seen (Fig. 7d).

The most likely reason for variable GABA content is a frameshift mutation that results in the elongation of unexpected peptides in place of CaMBD. In comparison to B and A type plants, the rice grain of the C type plant (GE 1: truncation of CaMBD) produced the highest GABA concentration; as a result, these plants were examined further in T_2 generation. Additionally, we examined T1 seeds from the #11, #14, and #26 lines among C type plants. Among these, line number #14 (designated as #14-1) had the highest GABA content (0.57 nmol/mg), compared to lines #11 (0.40 nmol/mg) and #26 (0.43 nmol/mg).

Thus, the mutant line #14-1, which matches the amino acid sequence of GE1 in Fig. 7c and has the nucleotide sequence no. 1 in Fig. 7b, was chosen to utilize in the next studies. Additionally, to assess the impact of truncation on phenotypic attributes and stress response, another mutant line, #14-6, was selected. This line was generated from small deletions of 14 bp and 8 bp independently at the CaMBD-coding area, as indicated in no. 6 in Fig. 7b. The result was a 53 amino acid polypeptide chain (GE 6 in Fig. 7c).

2.3.5 *In vitro* enzyme activity from total protein extracted from WT, #14-1 and #14-6 seeds

To investigate the enzymatic activity of GAD at physiological pH levels with or without Ca^{2+}/CaM, we extracted a crude protein extract from rice germ and used it in the GAD enzymatic procedure. In comparison to both its intact authentic extract (Ni) and #14-6, the crude protein of #14-1 had higher GAD activity, which might be attributed to the enhanced activity of GAD4ΔC in #14-1 (Fig. 7e). Ca^{2+}/CaM induced 1.3-fold greater activity in wild-type Ni at physiological pH (pH 7), but GAD activity was higher in #14-1 in the presence or absence of Ca^{2+}/CaM. In comparison to the wild-type control without Ca^{2+}/CaM, GAD activity rose 2.3- and 2.2-fold in #14-1 at pH 7 in the presence or absence of Ca^{2+}/CaM. It can be inferred that *Os*GAD4's C-terminal domain serves as a putative autoinhibitory domain. Consequently, truncating this region causes the enzyme to behave constitutively and exhibit higher activity. However, GAD activity in #14-6 was nearly identical to that of wild-type Ni. Notably, compared to when Ca^{2+}/CaM was absent, there was a trend towards an increase in GAD enzymatic activity in Ni wild-type seeds. The result indicates that the upregulated enzymatic activity of *Os*GAD4 in the truncated GAD4 mutant (#14-1) is the result of truncation of the C-terminal of the CaMBD.

2.3.6 Measurement of free amino acids

The gas chromatography/mass spectrometry (GC/MS) method is used for the quantitative analysis of free amino acids. The concentration of free amino acids (T_2 generation) was measured using gas chromatography-mass spectrometry (GC/MS) (Table 5). The quantities of Asn and Trp were significantly lower in the #14-1 line compared with the wild-type, whereas most other free amino acid levels were increased. Among the proteinaceous amino acids, the accumulation of Val, Ile, Leu, Glu, and Phe was significantly higher compared with wild-type Ni. The highest GABA content was found in line #14-1, which was almost 9 times higher compared with wild-type Ni. However, the other mutant #14-6 yielded much lower GABA than the wild-type but was found to produce significantly higher Leu, Pro, and Glu.

Amino acid	Ni	#14-1	#14-6
Ala	56.1 ± 4.1	113.2 ± 7.1** (2.0)	72 ± 11.7 (1.3)
Gly	15.9 ± 8.3	24.8 ± 1.6 (1.6)	12.5 ± 3.7 (0.8)
Val	7.3 ± 0.8	39.1 ± 2.1** (5.4)	11.9 ± 5.2 (1.6)
Leu	2.4 ± 0.6	12.9 ± 0.2** (5.3)	12.6 ± 1.6** (5.2)
Ile	2.3 ± 0.1	12.2 ± 0.4** (5.4)	6.6 ± 2.4* (2.9)
Ser	15.9 ± 1.5	31.1 ± 1.6** (2.0)	15.1 ± 1.8 (0.9)
Pro	13.7 ± 2.8	8.7 ± 3.8 (0.6)	34.9 ± 6.1** (4.0)
Asn	134.2 ± 15.0	44.8 ± 12.1** (0.3)	128.6 ± 26.4 (1.0)
Asp	92.1 ± 26.0	271.4 ± 21.6** (2.9)	141.7 ± 51.5 (1.5)
Met	42.4 ± 7.1	110.3 ± 9.7** (2.6)	59.7 ± 10.7* (1.4)
Glu	149.0 ± 7.8	804.6 ± 32.2** (5.4)	313.3 ± 20.7** (2.1)
Phe	2.1 ± 0.1	9.6 ± 1.0** (4.5)	16.7 ± 5.7* (7.8)
Gln	22.2 ± 1.6	48.0 ± 4.4* (2.2)	27.9 ± 4.7 (1.3)
His	17.7 ± 2.4	76.8 ± 9.1** (4.3)	18.2 ± 7.6 (1.0)
Tyr	7.6 ± 5.0	2.3 ± 1.2 (0.3)	6.0 ± 1.9 (0.8)
Trp	8.6 ± 1.0	1.7 ± 0.4** (0.2)	1.6 ± 0.6** (0.2)
GABA	14.7 ± 1.2	129.8 ± 20.9** (8.8)	11.3 ± 3.0 (0.8)

Value: average ± standard deviation (SD); data comprise of three biological replicates
*$P < 0.05$, **$P < 0.01$ versus Ni control; Data in parentheses are fold change in comparison to wild-type Ni.

Table 5. The concentration of each free amino acid in rice grain was determined by gas chromatography/mass spectrometry (GC/MS) and compared with wild-type Nipponbare.

2.3.7 Agricultural traits comparison

Genome editing allows precise alterations at specific loci in the plant genome, thus causing the alteration of agricultural traits in rice. However, agricultural statistics on rice harvests after genome editing might differ depending on the exact genetic alterations applied, the growing circumstances, and the agricultural techniques used. We collected agricultural data considering multiple morphological characters to compare the phenotype of the genome-edited line (GABA-enriched version) #14-1 with the wild-type.

Rice line	Dry weight (g)	No. of branch	Size of leaf blade (cm)	No. of panicle	Total weight of seeds (g)	Weight of 1000 seeds (g)	Culm length (cm)	Panicle length (cm)	No. of seeds per panicle
Ni	175 ± 7.1	40.5 ± 6.0	64.4 ± 1.2	37.3 ± 3.9	125.9 ± 4.9	26.8 ± 1.5	68.8 ± 5.1	19.6 ± 1.5	119.9 ± 8.5
#14-1	152.8 ± 9.2**	50.3 ± 5.6*	57.2 ± 2.9*	46.4 ± 4.8**	130.0± 5.7	23.0 ± 1.0*	62.3 ± 3.1*	19.1 ± 1.0	117.5 ± 11.8

Rice line	Ripening rate (%)	Heading date	50% flowering	>80% flowering	Pollen diameter (µm)	Pollen fertility rate (%)	Shedding rate (%)	Germination rate (%)
Ni	92.52 ± 2.9	2023.08.07	2023.08.14	2023.08.18	46.5 ± 0.5	97.8 ± 0.8	0.05 ± 0.02	100 ± 0.0
#14-1	72.9 ± 4.1**	2023.08.10	2023.08.20	2023.08.27	45.4± 0.3	96.6 ± 0.5	0.06 ± 0.01	97.2 ± 4.7

Table 6. Agricultural data of wild-type and genome-edited rice. They were grown in greenhouse conditions in the year 2023.

From agricultural trait analysis, we found out the genome-edited line #14-1 was a short-statured plant type producing a significantly higher number of panicles in comparison to the wild type. On the other hand, the ripening rate was less in #14-1 than the wild-type. Considering the morphological traits, it can be assumed that there is no aberrant phenotypic character in genome-edited plants. However, agricultural data is critical for assessing the efficacy, safety, and sustainability of genome-edited rice cultivars.

2.4 Discussion

GABA-enriched rice plants were produced for the current investigation. The *OsGAD4* gene's CaMBD coding region was truncated via CRISPR/Cas9-mediated genome editing. The basis for predicting the potential characteristics of *Os*GAD4, such as its authentic CaMBD and Ca^{2+}/CaM-induced activation, was established by comparing the C-terminal regions of plant GADs (Fig. 3a). Though *Os*GAD2 mutants lacking the C-terminal extension showed greater GABA levels but were unable to bind CaM, previous research with *Os*GAD1 demonstrated that it can bind to CaM (Akama et al. 2001; Akama and Takaiwa 2007). Apart from rice, the unique structure of GADs devoid of an authentic CaMBD has been confirmed in tea and apples (Trobacher et al. 2013; Mei et al. 2016). *Os*GAD2 and *Cs*GAD2 are unable to bind Ca^{2+}/CaM and are not triggered by CaM due to the absence of two or more critical residues in *Ph*GAD compared with real GAD (Fig. 3b) (Akama et al. 2001; Mei et al. 2016). Compared to wild-type rice grains, truncation of *Os*GAD3's C-terminal coding domain caused a seven-fold increase in GABA accumulation (Akama et al. 2020). It was proved that *Os*GAD4 is a Ca^{2+}/CaM-dependent enzyme that can bind to Ca^{2+}/CaM, as demonstrated by *in vitro* experiments (Fig. 4).

Previously, the transgenic strategy for C-terminal deletion resulted in enhanced GABA content in several species, such as tobacco, tea, and tomato (Baum et al. 1996; Mei et al. 2016; Takayama et al. 2017). Therefore, we planned a complete truncation of the coding region for CaMBD using the CRISPR/Cas9 approach, employing *in vivo* mutagenesis. Upstream and downstream gRNAs were designed to obtain an intact deletion of the domain (Fig. 5b). We managed to establish 27 lines (T_0), among which we selected 10 candidate lines (Fig. 6b). Out of these candidate lines (259 seedlings) which were analyzed at the DNA level, 70 seedlings (Table 4b) contained the expected 216 bp deletion (27% of total). The remaining lines were found with a variable number of base insertions or simultaneous insertions and deletions resulting in different polypeptide chain (Fig. 7b-c).

Variable GABA content, or phenotypic difference, was seen in the lines with various nucleotide sequences (Fig. 7d). This could be due to a variety of factors, including the development of a modified protein that is entirely different from CaMBD, which is one possible source of a frameshift mutation. Different lengths and functionalities of the protein are derived from various patterns of InDels in the sequences. Proteins that have been altered may be less able to repress the GAD enzyme's autoinhibition. Except for the intact truncated form of CaMBD, it may independently control the GABA biosynthesis in these mutants and result in GABA levels that are either lower or almost similar to those of the wild-type. Likewise, Nonaka et al. (2017) found that in tomato GAD3 genome-edited mutants, frameshift mutations slightly upstream of the CaMBD-coding sequence commonly resulted in an extension of changed peptides, with the majority exhibiting the same level of GABA accumulation as wild-type.

In a previous *OsGAD3* study, 41% of the lines exhibited shorter alterations while the remaining lines had the intended truncation of 122 bp (Akama et al. 2020). In contrast, single

insertions and simultaneous insertions and deletions made up the remaining changes in the tomato line where targeted mutagenesis resulted in deletions in 59.9% of the line, ranging from a single nucleotide to more than 200 nucleotides in the T_0 generation (Nonaka et al. 2017).

The GAD enzymatic activity data showed that wild-type Ni increased 1.3-fold with GAD activity modulated by Ca^{2+}/CaM, while GAD activity at pH 7.0 increased 2.3- and 2.2-fold, respectively, with truncation of the CaMBD from *Os*GAD4 (Fig. 7e). Because of a smaller deletion in the CaMBD coding area, which may interfere with crucial residues needed for the GAD and calmodulin interaction, decreased GAD activity in #14-6 may be seen. In contrast to Ni and #14-6, #14-1 exhibited much higher enzymatic activity, according to the results of the ANOVA. On the other hand, there was no statistically significant difference in GAD activity between any genotype when Ca^{2+}/CaM was present. An *Os*GAD2 truncated mutant's crude protein extracts showed extreme enzymatic activity compared to the wild type. Moreover, another study reported a rise in activities in truncated tomato GADs at C-terminal positions, GAD3ΔC; 16-fold at pH 7.0 compared with the full-length tomato GAD (Nonaka et al. 2017). According to these findings, *Sl*GAD3's C-terminal extension region, like that of other plant GADs (Baum et al. 1996; Akama and Takaiwa 2007), also serves as an autoinhibitory domain. Furthermore, the activity of these enzymes in other plant species, such as apples, increased once the C-terminal extension in GADs was removed (Trobacher et al. 2013). Therefore, it is likely that GAD activity is increased in neutral pH conditions in a Ca^{2+}/CaM -dependent way, as evidenced by the significantly higher activity of the truncated version of *Os*GAD4.

As expected, line #14-1 yielded about nine times the amount of GABA in brown rice compared to the wild-type Ni (Table 5). Except for Pro, Asn, Tyr, and Trp, most amino acids were found to be elevated in the genome-edited line in our investigation. These enhancements in the examined amino acids appeared to be about proportionate to GABA and closely related to those of GABA. Conversely, it was found that lines #14-6 produced nearly identical amounts of amino acids and less GABA than the wild type, but surprisingly, they also produced larger concentrations of Leu, Pro, and Glu. Similar outcomes were also observed by Akama et al. (2020) in a transgenic line with a single base deletion and a truncated C-terminal region of CaMBD, GAD3ΔC. As sink organs, rice grains' accumulation of GABA may have varying effects on the pool's amino acid composition (Akama et al. 2009). There may be a link between GABA and amino acid accumulation since an increase in GABA levels in rice grains may cause the buildup of other free amino acids. The creation of transgenic tomato fruits with antisense-suppressed GAD expression was documented by Kisaka et al. (2006). An analysis of the fruit's amino acids revealed an increase in Glu and other free amino acids in three of the four transgenic lines. It appears that genetic alteration of the GABA shunt in rice can lead to stable and high levels of GABA accumulation in the rice kernels along with an increase in other amino acids. The alteration of GABA biosynthesis and catabolism in rice, namely the suppression of GABA-transaminase (GABA-T), was the cause of the steady accumulation of GABA and other amino acids in the edible sections of the rice (Shimajiri et al. 2013a).

Nonaka et al. (2007) showed the modification of two *SlGAD* genes using the CRISPR/Cas9 method to delete the CaMBD coding region. Their targeted mutagenesis in tomato fruits showed seven- to fifteen-fold higher GABA buildup compared to wild-type. In the current study, genome-edited rice (#14-1) produced GABA levels nearly nine times greater than wild-type rice. On the other hand, GABA accumulation in rice grains increased seven-fold when *Os*GAD3's C-terminal truncation took place (Akama et al. 2020). GABA synthesis varied in rice GAD3 and GAD4, which underwent identical genome editing techniques. This may be because distinct transcriptional regulators or signaling molecules, for instance, might alter the GAD gene's expression or activity. Research revealed that rice seeds have higher levels of GAD3 transcription than GAD1 or GAD2 (Liu et al. 2005).

2.5 Conclusion and Future Perspective

We successfully utilized CRISPR/Cas9, a genome editing technique, to truncate the coding region of *Os*GAD4 at its C-terminal. In comparison to Nipponbare of the wild-type, our genome-edited rice strain generated GABA content that was nearly nine times greater. Increased intracellular GABA may enhance a plant's ability to withstand stress by triggering the activation of genes linked to metabolism and signaling that are important in controlling a plant's vigor and growth. Plant resilience to abiotic stress was enhanced by beneficial regulation of the GABA shunt and associated pathways (Bao et al., 2015). Transgenic plants are assumed to have accumulated extraordinarily high levels of intracellular GABA through the use of stress-inducible promoters or promoters specific to particular tissues or stages (Renault et al., 2011). Further understanding of this type of research would aid in the investigation of GABA function. Furthermore, rice grains with high GABA concentrations have the potential to become a popular GABA supplement meal for everyday consumption. Hence, we plan to investigate the function and expression of *OsGAD4* in the next study.

Chapter III
Evaluation of abiotic stress tolerance of truncated mutant

3.1 Introduction

Abiotic stressors such as drought, salt, severe temperatures, and water logging are crucial restraints on agricultural yield and food security globally. These abiotic stresses and climate change, as well as people's damaging actions, have all harmed cultivated lands which will result in scarcity of food (Zafar et al. 2020). With climate change worsening these calamities, there is an urgent need to create crop types that are more resistant to abiotic stress conditions. Genome editing technologies, notably CRISPR/Cas9, provide intriguing opportunities for targeted and precise crop genome alteration to improve stress resistance. This technology has enormous potential to produce genome-edited crop plants tolerant to multiple stresses by targeting numerous stress-sensitive genes concurrently in an elite high-yielding, but sensitive cultivar, and tolerance genes can also be overexpressed using CRISPR-mediated gene activation (Zafar et al. 2020). Researchers have been working to create crop types with increased tolerance to abiotic challenges by inserting precise mutations or deletions in critical regulatory genes that do not introduce undesirable genetic alterations. For instance, knock out of *SlLBD40* (lateral organ boundaries domain transcription factor) in tomato plants improves drought tolerance (Liu et al. 2020), while *WRKY3* and *WRKY4* genes help in drought resistance in *Arabidopsis* (Li et al. 2021).

Moreover, the prior study revealed that knocking out genes (AtWRKY3 and AtWRKY4) in *A. thaliana* creates salinity sensitivity by causing more ion escape along with lower antioxidant actions (Chen et al. 2021). On the other hand, CRISPR-mutants in rice by knocking out *OsDST* were found to survive salt stress (Santosh Kumar et al. 2020). This chapter will assess the abiotic stress tolerance of the truncated genome-edited mutant created utilizing CRISPR/Cas9 technology. However, the assessment of genome-edited mutants' performance under abiotic stress conditions is essential to assess their potential for practical application in agriculture. Since the C-terminal truncation of *OsGAD4* results in constitutive activation of GAD, which raises GABA levels constantly, it is anticipated that this mutant will be more resilient to abiotic stressors than wild-type plants. The increased levels of GABA offer multiple defense mechanisms, including osmotic adjustment, pH regulation, ROS scavenging, and metabolic integration. These mechanisms work together to improve the plant's resistance to a range of abiotic stressors.

The evaluation of stress tolerance included extensive investigations of the mutant's physiological, and molecular responses under controlled stress circumstances. Phenotypic variables like biomass change, survival rate, stress-related morphological alterations, and molecular response were assessed to identify the mutant's performance under various stress conditions.

3.2 Materials and Method

3.2.1 Abiotic stress experiments

We compared the expression data of five GAD genes (retrieved from the TENOR database) before the execution of abiotic stress experiments. Out of the five GAD genes, it is clear from the comparison that *OsGAD4* is highly expressed in multiple abiotic stress conditions. For instance, data retrieved from the Transcriptome ENcyclopedia Of Rice (TENOR) database clearly indicate the highest expression level of *OsGAD4* compared to other rice *GAD* genes when exposed to salinity stress (Fig. 8).

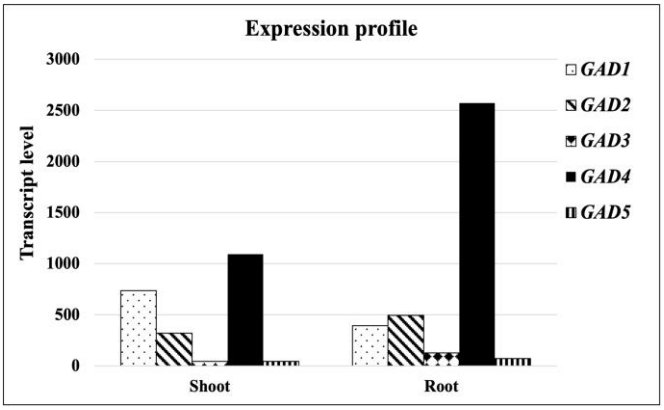

Figure 8. Expression analysis data of the five *OsGAD* genes under salinity stress condition. Data was retrieved from TENOR database (https://tenor.dna.affrc.go.jp/). Values indicate the transcript levels of shoot and root tissues of rice seedlings.

Rice seeds from lines #14-6 (small deletion at the CaMBD-coding region) and #14-1 (C-terminal truncated version of CaMBD of *Os*GAD4) were germinated and allowed to grow for two weeks in Petri dishes containing 0.5 X MS media inside a growth chamber at 25°C with a 16 h light/8 h dark period. This was done in preparation to induce stress *in vitro*. Next, salinity, flooding, and drought conditions were applied to the seedlings (Ni, #14-1, and #14-6 in each stress). Plants were kept in a 150 mM NaCl solution for 0, 1, 3, and 6 hours to induce salt stress. For use in future research, samples of the vegetative tissues (root and shoot) were frozen in liquid nitrogen and kept at -80°C. The seedlings were completely submerged in liquid MS media to apply flooding stress, and comparable time-lapse treatments (0, 1, 3, and 6 h) were performed to prepare samples. Conversely, a longer stress duration of 0, 1, 3, 6, 12, and 24 hours was used to test the induction of responses against drought stress. Drought stress was imposed by removing the plants from growing media and kept in room temperature.

Furthermore, the survival rate as the indicator of abiotic stress tolerance of the wild-type and mutant rice plants was checked by increasing the duration and strength of adversity. After being exposed to high-salt treatment stress for two days in a 150 mM NaCl solution, the seedlings were allowed to grow in small pots with soil (Green soil, Japan Agriculture group) under normal conditions for a further seventeen days. In the event of flooding stress, plants were immersed in the nearly hypoxic conditions of 1X MS (liquid) media after 3 days and

allowed to grow normally for an additional 17 days. The plants were subjected to drought stress by being taken off from growth media and placed on a petri plate in the open at room temperature until the fresh weight of the wild-type plant (Ni) dropped by about 25%. The plants were then grown for 17 days, like the other stress-treated plants to determine the survival rate, after being rehydrated for 3 hours to aid in recovery. Additionally, fresh weights of stress-surviving plants were recorded, and they were then dried overnight in an oven at 48 °C before their dry weights were measured the following day to do biomass comparisons.

3.2.2 Amino acids isolation and GABA content measurement

The sample was collected at various time points as described above and then amino acid was isolated and GABase enzymatic assay was performed as mentioned in previous chapter.

3.2.3 RNA isolation

The plant material (leaf and stem), ~50mg was collected from each plants at vegetative stage. Then it was frozen on liquid nitrogen and crushed in tubes containing small (5mm) stainless steel beads. Total RNA was isolated using the TRISURE (Bioline, Germany) Total RNA isolation reagent protocol:

- 1ml TRISURE reagent was added to the plant material (homogenized samples) and incubated for 5 min at room temperature.
- 200µl chloroform was added, shaken for 15 sec, and incubated for 3 min at room temperature.
- Centrifuged at 12,000 x *g* for 5 min at 4ºC.
- The supernatant was transferred to a clean tube and precipitated the RNA by adding 700µl cold isopropanol.
- Incubated for 10 min at room temperature and centrifuged for 20 min at 14,000 x *g*, 4ºC.
- RNA pellet was washed in 1ml 70% cold ethanol and centrifuged for 5 min at 14,000 x *g*, 4ºC.
- The RNA pellets were dried and dissolved in 50 µl in RNase-free DEPC (diethylpyrocarbonate)-treated H_2O for 10 min.
- The RNA intactness was confirmed by comparison to the fragment intensities in electrophoresis of the individual samples on 1.5% agarose gel.

DNase I treatment

The RNA samples were treated with DNase I (10 unit/µl) (Roche, Germany) at 37 ºC for 1 h to ensure no genomic DNA was left in the samples. 45µl total RNA from each sample was treated with the following solution.

- A 100 µl reaction containing the following ingredients:

- 45 µl RNA
- 10 µl of 10x DNaseI buffer (30 units)
- 1 µl DNase I
-0.5 µl RNase inhibitor

Volume adjusted to 100 µl with RNase-free water and incubated at 37 ºC for 60 min.

- 100µl of phenol: Chloroform: isoamylalcohol = 25:24:1 was added and mixed well
- Centrifuged for 10 min at 14,000 x *g* at 4ºC and transferred the RNA to a clean tube.
- Washed with 10 µl of 3M sodium acetate (pH 5.2) and 250 µl of 100% ethanol
- Centrifuged 20 min at 14,000 x *g* at 4ºC and discarded ethanol
- Again, the RNA pellet was washed with 70% ethanol
- Dried the RNA and dissolved in 100 µl RNase-free water

Then mixed well and ready for storage at -80ºC

Determination of the RNA concentrations in the samples was done based on values given by measurement on a Qubit (Flurometer) (RNA BR Assay kit, Invitrogen, Thermo Fisher Scientific, USA) in two parallel sample dilutions.

3.2.4 cDNA synthesis

Complementary DNA, cDNA, was synthesized using reverse transcriptase (RT) reaction. Reverse transcriptase is an enzyme that translates RNA to DNA. This creates one DNA (cDNA) strand complementary to the RNA strand in a DNA-RNA hybrid. In this case, total RNA was isolated and used as a template for cDNA synthesis. The mRNA (which makes up 1-5% of the total RNA) is an essential fragment for the expression study.

- The following reaction mixture (volume 20 µl) was added to the extracted total RNA amounts to each sample:

- 4 µl 5X RT buffer
- 2 µl 10 mM dNTP
-1 µl Oligo dT Primer (5 pmol/µl)
-1 µl RT Ace (Toyobo)
- 0.4 µl RNase I Inhibitor (Toyobo, Japan)
-RNA, X (RNA= X/ 2000 ng, X= concentration of RNA)
-RNase-free water, Y (to adjust the volume up to 20 µl)

- Incubated at 42ºC for 60 min.
- Terminated the reactions at 99ºC for 5 min and chilled on ice.

3.2.5 RT-qPCR (Reverse Transcriptase –quantitative Polymerase Chain Reaction)

Template (cDNA) – 2 µl
10X Taq buffer - 2 µl
dNTP (10 mM) - 2 µl
Primer F1 -1 µl and Primer R356 – 1 µl (Table 2)
Taq DNA polymerase - 0.2 µl

RNase-free water was added to adjust the volume.
PCR condition:
Denaturation (95ºC, 30S),
Annealing (60ºC, 30S),
Extension (72ºC, 30S) and 30 cycle

cDNAs were used for RT-qPCR analysis in an ECO Real-Time PCR System (PCR max, United Kingdom). As an internal control, TATA-binding protein 2 (TBP2) was amplified with primers TBP2-F and TBP2-R. The results of RT-qPCR were calculated using the $2^{-\Delta\Delta CT}$ method (Livak and Schmittgen 2001).

3.2.6 Measurement of antioxidant enzyme activity

The highly responsive time points of each stress were considered for checking antioxidant enzyme activity. After stress treatment of two weeks old rice seedlings, leaf samples (200 mg) were collected in liquid N_2, and then homogenized in 2.0 mL of extraction buffer containing 100 mM potassium phosphate (pH 7.8), 0.1 mM ethylenediaminetetraacetic acid (EDTA), and 10 mM ascorbic acid. The homogenate was centrifuged at 14,000 x *g* for 15 minutes at 4°C. The supernatant was collected to measure the activities of Peroxidase (POD), Catalase (CAT), and Ascorbate peroxidase (APX) activity.

CAT activity was measured following the protocol developed by Azevedo et al. (1998) with some modifications. Its activity was measured using a spectrophotometer that measured H_2O_2 degradation at 240 nm for 2 minutes in a reaction medium comprising 100 mM potassium phosphate buffer (pH 7.0), 12.5 mM H_2O_2, and 50 µL of plant extract incubated at 28 degrees Celsius. As a blank solution, the same reaction media without plant extract was used. The activity of the CAT enzyme was measured in l mol H_2O_2 min^{-1} mg^{-1} of protein. Besides, the activity of APX was measured using Nakano and Asada's (1981) method of detecting ascorbate oxidation at 290 nm. The reaction medium was incubated at 28 degrees Celsius. It included 100 mM potassium phosphate buffer (pH 7.0), 0.5 mM ascorbic acid, and 0.1 mM H_2O_2. The reduction in absorbance was measured for 2 minutes after the reaction began, and APX activity was represented as l mol ASC min^{-1} mg^{-1} of protein. Moreover, POD activity was determined using the procedures of Bai et al. (2009). The solution for the POD activity measurement contained 50 mM (pH 7.8) phosphate buffer, 25 mM guaiacol, 20 mM (H_2O_2) and 0.50 ml of a 3 ml enzyme extract reaction solution. One unit of POD activity was expressed as a 0.01- unit/min shift in absorbance.

3.2.7 DAB (3,3'-diaminobenzidine) staining

For the DAB staining assay, the seedlings were treated with a specific period of stress treatment such as 1 h for flood stress, 6h for salinity, and 24 h for drought stress. At the same time, untreated control was maintained. After that, the 2nd leaf of each plant was excised and subjected to DAB staining. The leaves were incubated in a DAB (0.1% [w/v] DAB, 10 mM Na_2HPO_4, 0.05% Tween 20, pH 3.8) solution overnight at room temperature (25°C). After staining, the leaves were soaked in 95% ethanol overnight to remove chlorophyll.

3.2.8 RNA-seq analysis in drought stress experiment

Among the stress conditions evaluated, drought stress showed a much stronger stress response in terms of GABA accumulation and mRNA expression level. Hence, drought sample (after 24 h of treatment) was selected for RNA-seq analysis.

3.2.8.1 Mapping reads to the reference genome

The reference genome and gene model annotation files were downloaded from the genome website directly. Hisat2 v2.0.5 was used to create the reference genome index and to match paired-end clean reads to the reference genome. Hisat2 (Mortazavi et al. 2008) was chosen as the mapping tool because it can construct a database of splice junctions based on the gene model annotation file.

3.2.8.2 Quantification of gene expression level

FeatureCounts (Liao et al. 2014) v1.5.0-p3 was used to count the reads numbers mapped to each gene. Then FPKM of each gene was calculated based on the length of the gene and the reads count mapped to this gene. FPKM, expected number of Fragments Per Kilobase of transcript sequence per Millions base pairs sequenced. It considers the effect of sequencing depth and gene length for the reads count at the same time and is currently the most commonly used method for estimating gene expression levels.

3.2.8.3 Differential expression analysis

Before differential gene expression analysis, for each sequenced library, the read counts were adjusted by the edgeR program package through one scaling normalized factor. Differential expression analysis of two conditions was performed using edge R package (3.22.5). The *P* values were adjusted using the Benjamini & Hochberg method. Corrected *P*-value of 0.05 and absolute fold-change of 2 were set as the threshold for significantly differential expression.

3.2.8.4 GO, KEGG enrichment analysis of differentially expressed genes

Gene Ontology (Young et al. 2010) (GO) enrichment analysis of differentially expressed genes was implemented by the clusterProfiler R package, in which gene length bias was corrected. GO terms with corrected *P*-value less than 0.05 were considered significantly enriched by differentially expressed genes. KEGG is a database resource for understanding high-level functions and utilities of the biological system, such as the cell, the organism, and the ecosystem, from molecular-level information, especially large-scale molecular datasets generated by genome sequencing and other high-throughput experimental technologies (http://www.genome.jp/kegg/). clusterProfiler R package was used to test the statistical enrichment of differential expression genes in KEGG (Kanehisha and Goto 2000) pathways.

3.3 Results

3.3.1 Abiotic stress-induced the GABA accumulation in vegetative tissues

Previous research has shown that, although the rate of accumulation varies greatly, abiotic stressors raise endogenous GABA concentrations in plant tissues (Li et al. 2021). During the early vegetative stage, we observed the responses of rice seedlings to various stressors. First, a 150 mM NaCl salt solution was used *in vitro* to treat 2-week-old rice seedlings over a range of time points. Second, rice seedlings underwent flooding stress treatment by being fully submerged in a liquid MS medium. Lastly, seedlings of the same age were left to develop in a dehydrated state without any media for drought stress treatment.

Collected samples were used for amino acid isolation followed by GABA content measurement. After one hour of treatment, salt stress commenced accumulation of GABA in shoot tissues of line #14-1 that was greater than that of wild-type Ni (Fig. 9a). GABA levels were reduced after 3 h of treatment and climbed again at the highest point after 6 h of stress treatment, reaching 2.6-fold higher compared with wild-type Ni. In root tissues, GABA induction demonstrated a gradual increase with the duration of stress and rose to the maximum at 6 h, producing an extreme yield of almost 4.3-fold higher GABA levels compared with wild-type. On the contrary, #14-6 had shown a considerable increase in GABA content of root tissue after 3 h of salt treatment which was almost 1.4-fold in comparison to the wild type. In the case of flooding treatment, line #14-1's root tissues showed a sharp increase in GABA accumulation, which peaked at 1 h and was almost 3.3 times higher than that of wild-type Ni (Fig. 9b). GABA levels then started to drop after 3 and 6 h of flooding stress. Similar trends in GABA synthesis were observed in shoot tissues, resulting in noticeably elevated GABA levels after one hour. In both vegetative tissues (shoot and root), the flood stress response in the short deletion mutant (#14-6) was nearly as high as in the wild type.

a. Salinity

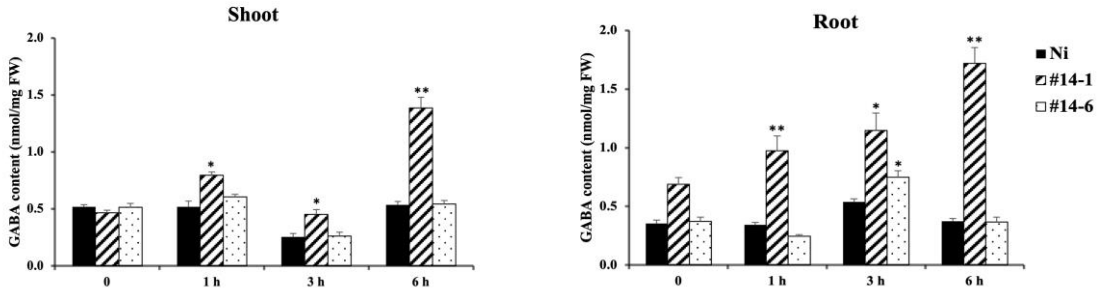

b. Flooding

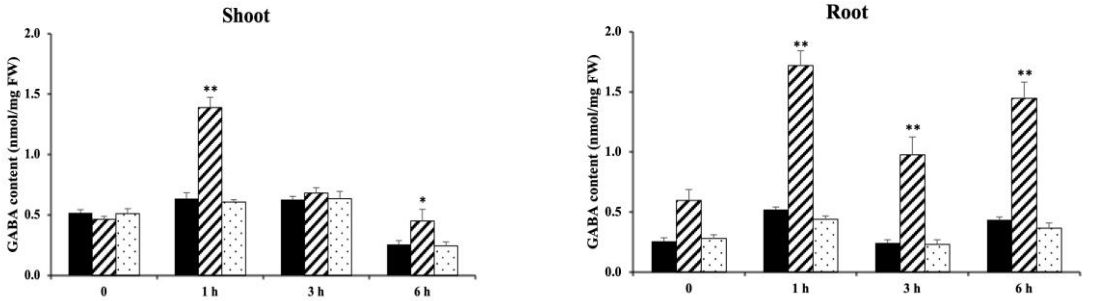

c. Drought

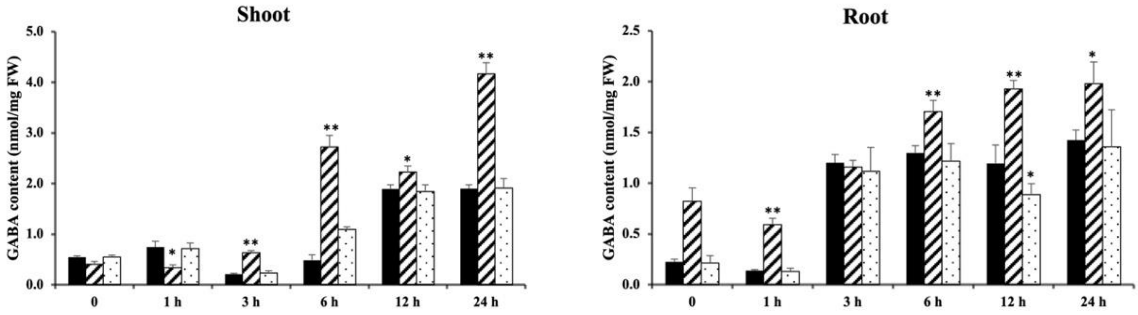

Figure 9. Response to abiotic stresses as GABA accretion.

a) GABA accumulation in vegetative tissues (shoot and root) of 2-week-old Ni, #14-1 and #14-6 seedlings when challenged with salinity. For salinity stress, plants were placed in 150 mM NaCl solution for a time course of 0, 1, 3, and 6 h. **b)** Flooding stress was implemented by complete submergence of the seedlings in liquid MS media and similar time interval treatments of 0, 1, 3, and 6 h, and **c)** Drought stress was carried out by removing the plants from the growing media and involved a longer duration of stress (0, 1, 3, 6, 12, and 24 h) to record the induction of response. Ni= wild-type control; #14-1= *OsGAD4* genome-edited plant with intact deletion of CaMBD; #14-6= *OsGAD4* genome-edited plant with short deletion in the coding region for CaMBD. Error bars indicate SD (n=3). Levels of significance were determined by comparing with the wild-type values in the same stress conditions. Asterisks indicate significant differences (*$P < 0.05$, **$P < 0.01$).

In addition, young rice seedlings were subjected to drought stress to assess the reaction in GABA accumulation trend. When shoot tissues were subjected to drought stress, GABA concentration increased beginning at 6 h, decreased slightly at 12 h, and then increased once more at 24 h (Fig. 9c). In comparison to the wild-type, line #14-1 generated GABA at a rate that was almost 2.2 times higher at this time. The line #14-6 also showed increased GABA buildup. In addition, drought stress induced the gradual increase of GABA build up over time in the root tissues of #14-1, peaking at 24 h. When considered together, it is evident that the induction of GABA in the vegetative tissues of young rice seedlings exhibited a diverse reaction to various abiotic stresses, and that the accumulation of GABA was increased in the vegetative tissues in response to abiotic stresses.

3.3.2 mRNA expression levels are upregulated in vegetative tissues upon exposure to abiotic stresses

Deciphering the molecular mechanisms behind stress responses, identifying genes and signaling pathways responsive to stress, comprehending stress tolerance mechanisms, and enhancing crop resilience to environmental challenges mostly depend on mRNA expression levels under abiotic stress conditions.

Reverse transcription-quantitative polymerase chain reaction (RT-qPCR) of vegetative tissues exposed to the same abiotic stresses as for GABA content measurement was performed at various times to investigate changes in the expression levels of *OsGAD4*. Despite having the same promoter region, the wild-type Ni, #14-1, and #14-6 that were examined here showed nearly comparable expression levels. When exposed to salt stress, mRNA expression levels of the root tissues were greatly increased at 1 h and subsequently somewhat decreased at 3 h (Fig. 10a). When compared to the untreated control, strong expression peaked up to 3.1 times after 6 h. In response to salt stress, shoot tissues also displayed consistent expression levels, but at comparatively lower levels at the same time point than root tissues.

a. Salinity

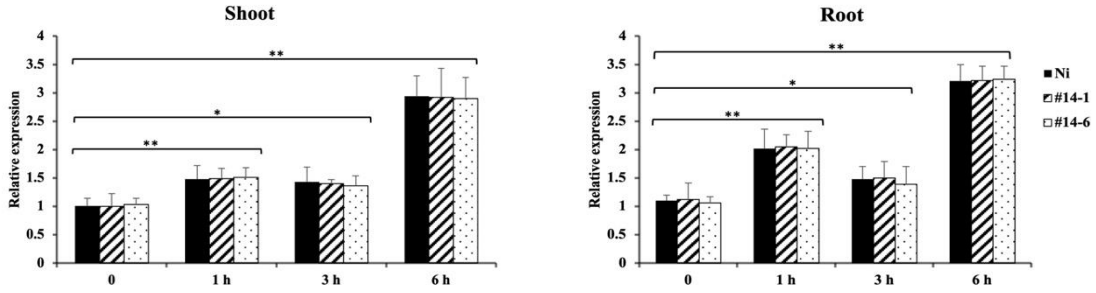

b. Flooding

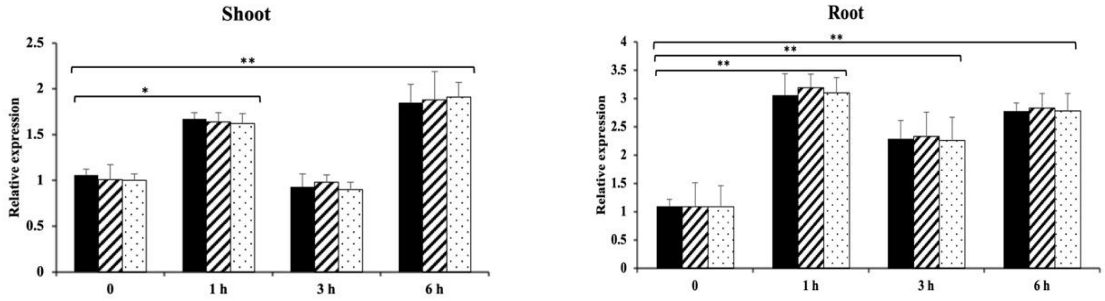

c. Drought

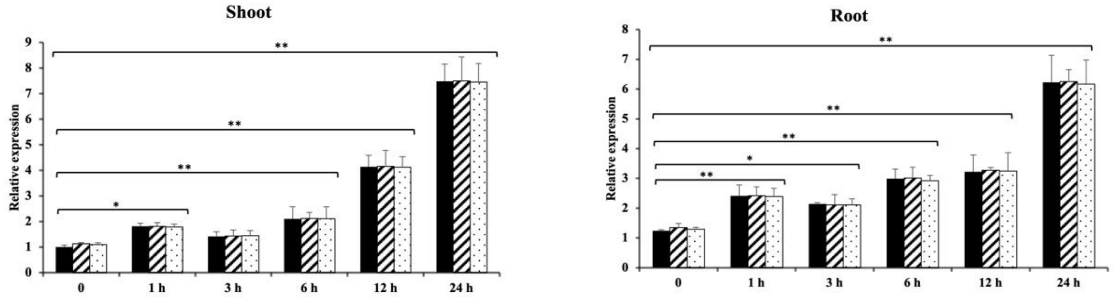

Figure 10. *OsGAD4* gene expression in response to abiotic stresses a) salinity, **b)** flooding, and **c)** drought in genome-edited rice plants. The stress treatments and durations are described in the text. The expression level was analyzed by RT-qPCR. TATA-binding protein 2 (TBP2) was used as an internal control. The relative expression level was analyzed using the $2^{-\Delta\Delta CT}$ method. Error bars indicate SD (n=3). Levels of significance were determined by comparing values of stress-treated samples to the respective non-stressed conditions. Asterisks indicate significant differences (*$P < 0.05$, **$P < 0.01$). The asterisk above the bar indicates the level of significance in three lines simultaneously compared to the non-stressed control.

When compared to the untreated control, root tissue had an approximately 3.1-fold increase in mRNA expression levels after flooding stress, which was shown to occur quickly at 1 h (Fig. 10b). Remarkably, despite levels being greater than the control, shoot tissues did not exhibit considerable upregulation under the same stress scenario. Following this time point, the expression in the root tissues marginally decreased for 3 h before increasing at 6 h.

Similar patterns were also seen in the shoot tissues, with mRNA expression showing a tendency to decrease at 3 h and then markedly increase at 6 h.

Concerning drought stress, both shoot and root tissues exhibited steady upregulation of expression at the onset of stress treatment at 1 h (Fig. 10c). At the 3 h time point, expression levels had a trend towards a decrease in shoot tissues, almost similar to untreated samples. However, root tissue showed increased expression at this point. Eventually, with an increase in duration of stress the expression level increased moderately and reached a maximum at 24 h. When compared to the untreated control, the rise in the shoot and root tissues was 7.5 and 6.3 times, respectively. Mostly our mRNA expression data supports the transcriptional activity or gene expression profile found in the TENOR database (Kawahara et al. 2016).

3.3.3 Abiotic stress tolerance was significantly improved in #14-1 rice plants

We compared the *OsGAD4* genome-edited plants' tolerance level to that of wild-type plants in response to salinity, flooding, and drought conditions. Multiple stressors were applied to two-week-old seedlings, as detailed in the materials and method section. Following the stress treatment, the seedlings were placed in small pots with soil after being cleaned and rehydrated for three hours (Fig. 11). C-terminal truncated line #14-1 showed salt stress tolerance when we used a 150 mM NaCl solution for 2 d in our experiment. Line #14-1 exhibited a survival rate of 44.2% when subjected to salt stress, while wild-type and #14-6 plants showed survival rates of 17.3% and 15.2%, respectively (Table 7). For flooding stress, 25.6% of wild-type plants survived, and line #14-1 showed a survival rate of 59.6%. Table 7 shows that of the line #14-1 seedlings, 34.5% of them survived the drought stress, whereas the wild-type line had a survival rate of just 12.2%, and line #14-6 had an even lower survival rate of 11.7%. Our findings demonstrated a significant improvement in abiotic stress tolerance during the early vegetative stage in the *Os*GAD4 genome-edited mutant of the truncated version of CaMBD.

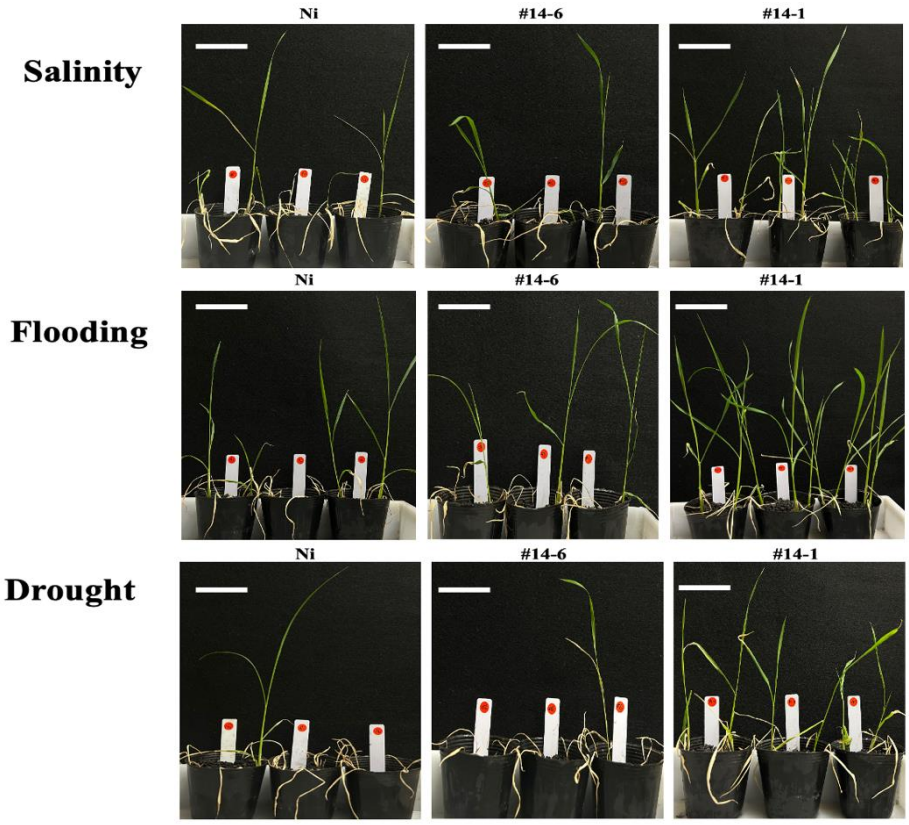

Figure 11. Abiotic stress (salinity, flooding, and drought) tolerance of wild-type, #14-1 and #14-6 seedlings at the early vegetative stage. The stress treatments were carried out as described in the text. High-salt treatment: 150 mM NaCl solution was used to dip the seedlings for 2 d and then removed from the high-salt conditions to grow for 17 d in small pots containing soil in normal conditions. Flooding stress: plants were allowed to stay immersed in liquid MS media for 3 d and thereafter removed and grown normally for another 17 d. Drought stress: the plants were removed from growth media and left on a petri dish in the open air and at room temperature until the fresh weight of the wild-type plant (Ni) was reduced to approximately 25% (6h). Afterward, plants were rehydrated and grown for 17 d. For each line, 12 seedlings were used in one replication of an individual experiment. Independent stress experiment was repeated at least 3 times. Scale bar=10 cm.

3.3.4 Comparison of biomass loss after stress treatment

We measured the fresh weight and dry weight of the surviving plants to compare their biomass. After removing from the soil, plants were washed to get rid of the dirt, the fresh weight was measured. The cleaned plant sample was dried overnight at 45°C in an oven to determine its dry weight. The results showed that under all these three stress situations, the biomass reduction as fresh weight in #14-1 plants was much less than that in wild-type plants (Table 7). In response to the abiotic stresses, wild-type plants showed greater dry weight loss than #14-1 plants did. This suggests that #14-1 plants have a defense mechanism that allows them to withstand the adverse environment. Biomass loss in #14-6 was found almost identical to the wild type articulating its inability to defend the plant against stress conditions.

Type of stress	Survival rate (%)			Biomass loss % (FW)			Biomass loss % (DW)		
	Ni	#14-6	#14-1	Ni	#14-6	#14-1	Ni	#14-6	#14-1
Salinity	17.3 ± 8.1	15.2 ± 10.0	44.2 ± 12.3**	33.1 ± 4.2	33.5 ± 7.4	10.8 ± 3.7**	27.9 ± 14.5	31.4 ± 9.5	10.2 ± 6.2*
Flooding	25.6 ± 6.3	21.3 ± 5.2	59.6 ± 20.1*	25.9 ± 7.8	28.0 ± 8.6	10.2 ± 1.7**	22.3 ± 8.4	23.8 ± 6.1	12.1 ± 7.9*
Drought	12.2 ± 4.8	11.7 ± 4.6	34.5 ± 9.7**	35.6 ± 4.2	36.7 ± 3.7	15.0 ± 3.3**	29.1 ± 4.0	29.4 ± 5.7	9.6 ± 1.8**

Table 7. Quantitative data on survival rate and biomass reduction after the seedlings survived abiotic stresses

DW=dry weight, FW=fresh weight. The values are calculated from averages of the surviving plants in each stress with wild-type, line #14-1 and line #14-6. The average number of surviving plants was converted to a percentage to show the survival rate. These data represent the combined result of two independent experiments each with three replications in each stress condition. In the case of biomass, the control or untreated fresh and dry weight was assumed as 100%. Biomass loss was calculated by deducting the biomass of stress-surviving plants from that of the untreated one. Asterisks indicate significant differences compared to wild-type (*$P < 0.05$, **$P < 0.01$).

According to our current findings, plants' ability to withstand abiotic stress may be linked to elevated GABA levels because they serve a protective function. GABA may operate as a stress-defense system by modulating other hormones that regulate stress. More research is necessary to understand the underlying mechanism.

3.3.5 The activity of antioxidant enzymes under abiotic stresses

CAT activity was increased significantly in the #14-1 line in response to salinity stress, but there was no significant increase in response to flood stress when compared to wild type and the other line #14-6 (Fig. 12a). It is worth noting that catalase activity showed a stronger reaction in response to salinity stress than drought stress. POD activity was highest in all the lines including #14-1 under drought stress among the three stress conditions considered (Fig. 12b). Salinity and flood stress also increased the POD antioxidant activity compared to the non-stress control condition. Furthermore, APX activity had a sharp rise in #14-1 against drought stress condition comparing the wild type (Fig.12c). Short deletion mutant #14-6 exhibited similar antioxidant enzyme activity to the wild type in all the stress conditions.

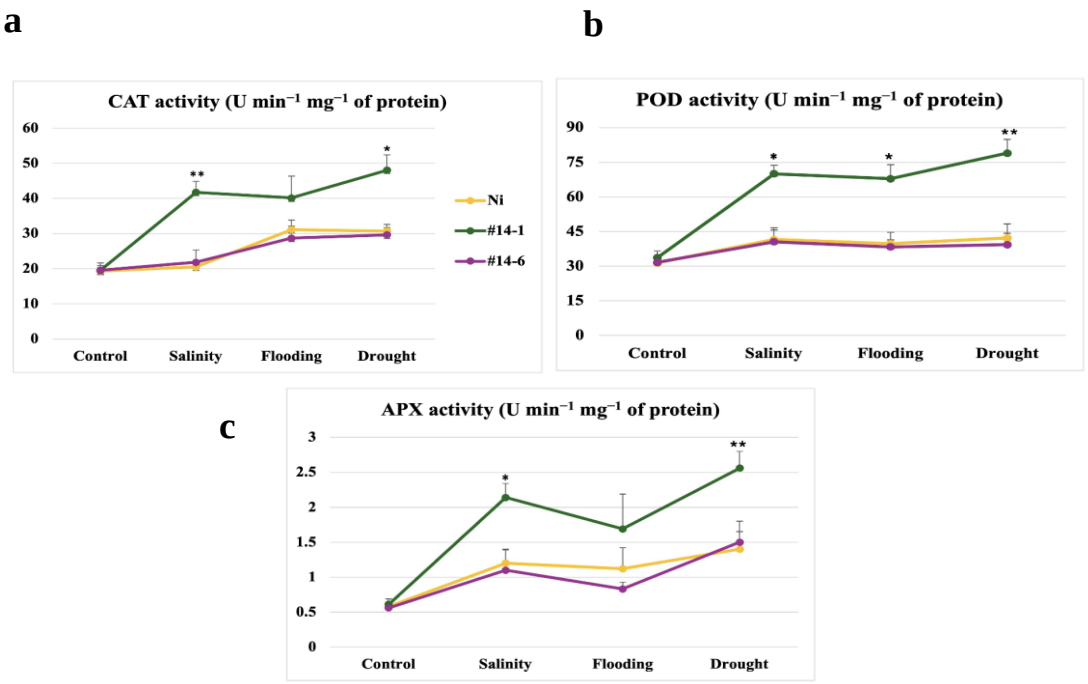

Figure 12. Activity of the antioxidant enzyme (a)Catalase (b)Peroxidase, (c)Ascorbate peroxidase. Rice plants of Ni, #14-1 and #14-6 were subjected to salinity, flooding and drought conditions.

3.3.6 DAB (3,3'-diaminobenzidine) staining of leaf tissues before and after selected stress treatment

DAB is a chromogenic substrate that reacts with H_2O_2 in the presence of peroxidase, resulting in the formation of a brown precipitate. The intensity of the brown color correlates with the amount of H_2O_2 present in the tissue. The accumulation of H_2O_2 is an indication of ROS production induced by multiple stress conditions, which results in oxidative damage. The flag leaves from salinity, flood, and drought stress-treated plants were extensively stained by DAB. The severity of staining or brown spots indicates the degree of H_2O_2 accumulation in the wild type Ni, #14-1 and #14-6. Rice leaves were more extensively stained by DAB under drought stress condition, followed by salinity and flood stress compared to the control condition (Fig. 13). However, the intensity of the DAB staining decreased in #14-1 plants under all stress conditions, suggesting the antagonistic mechanism of the line against ROS accumulation.

Histochemical analyses with 3,3′-diaminobenzidine (DAB) revealed that ROS accumulation was repressed to a certain extent in the C-terminal truncated version of *Os*GAD4 (#14-1) under abiotic stress conditions in rice leaves. These results suggest that endogenous GABA enhances abiotic stress tolerance by detoxifying ROS. In the current study, DAB staining shows the extreme H_2O_2 accumulation patterns in the leaves of plants under water deficit conditions, these data are associated with the trend of antioxidant enzyme activity.

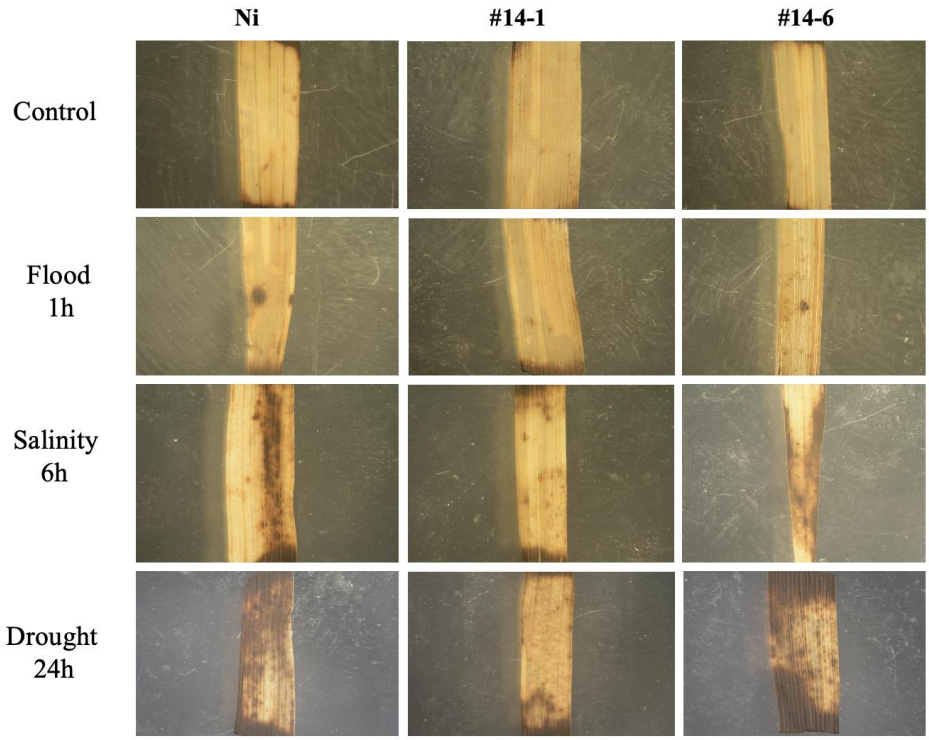

Figure 13. DAB staining of wild-type Ni, #14-1 and #14-6 leaves under normal conditions and abiotic stress treatment. Flood stress was applied for 1 h, salinity stress for 6 h, and drought stress for 24 h.

3.3.7 RNA-seq data on drought stress treatment

Drought is one of the devastating environmental stresses that affect plants' growth and development to certain extents and can be lethal at times. With global climate change, fluctuations in annual rainfall patterns, uneven distribution of rainfall during the rice-growing season, and inadequate rainfall in many locations all contribute to drought stress and detrimental effects on rice quality and yield. Drought stress reduces water intake, lessens photosynthetic efficiency, and disrupts several metabolic processes, including membrane transport, and metabolite formation. Among other staple crops rice is found to be particularly sensitive to drought stress throughout its entire life cycle (Panda et al., 2021). At this point, we narrow down our focus on drought stress to know the underlying mechanism of stress tolerance by RNA seq analysis. To do so, drought stress treatment was done with Ni wild type and C-terminal truncated version of *OsGAD4*; #14-1 for 24 h, and then samples were collected for total RNA isolation and further RNA-seq analysis. Along with drought stress samples, the control condition was also considered without any stress.

3.3.7.1 Co-expression Venn diagram

A co-expression Venn diagram is a graphical tool for representing the link between diverse groups of genes that co-express under different situations. The Venn diagram's intersections represent genes that are co-regulated and may share common regulatory mechanisms or functions, whereas the non-overlapping areas represent genes that are uniquely expressed under specific conditions, implying specialized roles in response to that particular stimulus. Researchers can learn about the intricate networks of gene regulation and the functional redundancy or specificity of genes within these networks by analysing the patterns of co-expression indicated by Venn diagrams.

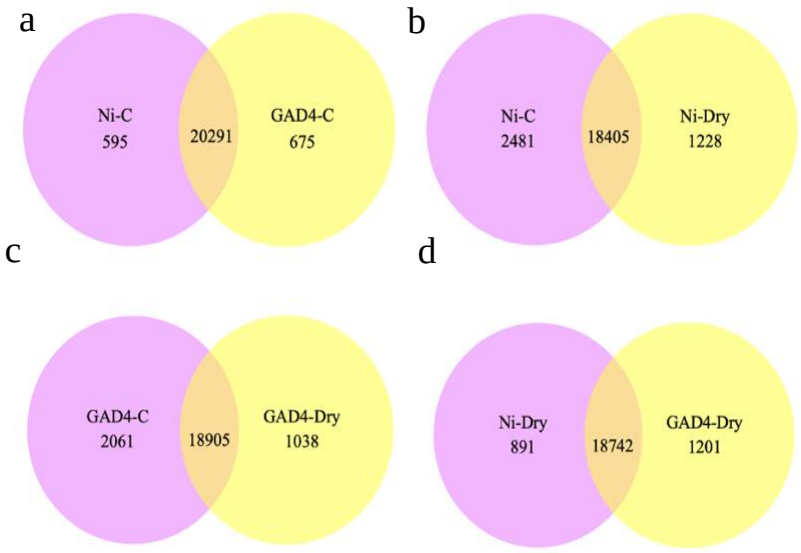

Figure 14. Venn diagram of differentially expressed genes. a) Ni-control and GAD4-control, b) Ni-control and Ni-dry, c) GAD4-control and GAD4-dry d) Ni-dry and GAD4-dry. Here, Ni-C= wild type control, Ni-Dry= wild type under drought, GAD4-C= #14-1 control and GAD4-Dry= #14-1 under drought.

The diagram shows the number of genes uniquely expressed and the overlapping region. No. of genes co-expressed in two samples, Ni control vs dry was 18405; on the other hand co-expressed gene in GAD4 control vs dry was 18905 (Fig. 14). Co-expressed gene was found higher in GAD4 compared to Ni. Again, the number of uniquely expressed gene in #14-1 was 675 (Fig. 14a) and 1201(Fig. 14d) in control and dry conditions respectively compared to the same condition of wild-type Ni, when compared to the same condition of wild type. This data indicates the regulatory importance of the uniquely expressed gene of GAD4 genome edited line in the stress response mechanism.

3.3.7.2 Differentially expressed gene statistics

The number of differentially expressed genes, which can be up- or down-regulated, reflects the amount of transcriptional change in an organism under certain conditions as compared to a control state.

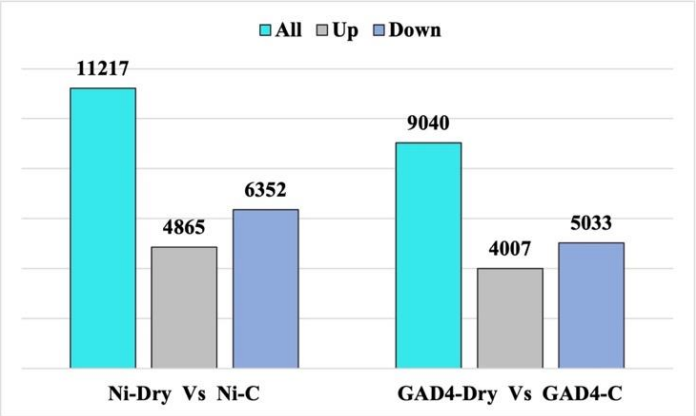

Figure 15. Comparison of upregulation and downregulation of differential genes.
Ni-dry vs Ni-c= comparison between control and drought stress condition of Ni, GAD4-dry vs GAD4-c= comparison between control and drought stress condition of #14-1.

The number of differential genes (including up-regulation and down-regulation) presented here in different groups. Comparison between up and downregulated gene Ni control vs Ni dry; GAD4 control vs GAD4 dry revealed that in all cases downregulated gene was higher (Fig. 15). However, down-regulation of genes denotes a reduction in the expression level of certain genes. A large number of down-regulated genes indicate that the organism is shutting down certain genes' functions, potentially to preserve energy, adapt to changes, or regulate mechanisms in response to multiple factors. The overall pattern of up- and down-regulation can aid researchers in understanding the biological processes impacted by the conditions under study, identifying prospective genes of interest for further investigation, and gaining insight into gene expression regulatory networks (Liu et al., 2014). The particular functions and consequences of these variations in gene expression might be complicated, depending on the context of the study and the biological system being investigated.

3.3.7.3 Gene Ontology (GO) enrichment analysis:

Gene Ontology (GO) enrichment analysis in RNA sequencing is a popular bioinformatics approach that helps researchers understand the functional importance of differentially expressed genes. It helps to analyze collections of genes or proteins by

detecting Gene Ontology terms that are significantly overrepresented in a particular set. GO terms are organized into three major categories: biological processes (BP), molecular functions (MF), and cellular components (CC).

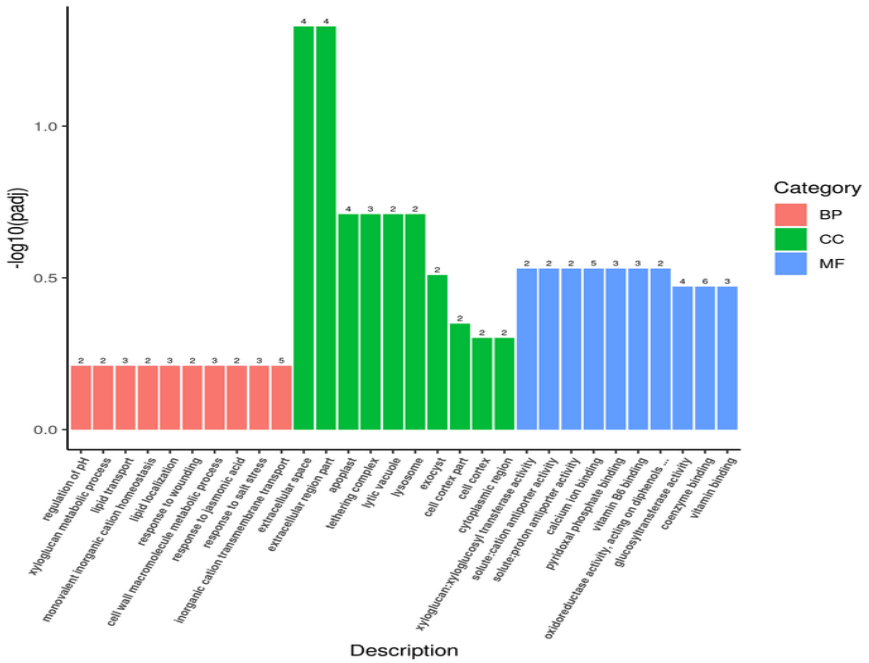

Figure 16. Gene Ontology (GO) enrichment analysis Of DEGs. GO analysis was done to compare the drought stress-responsive mechanism. The different colors represent the three GO subclasses of BP: biological process, CC: cellular component, MF: molecular function.

The gene responsible for “extracellular space” and “extracellular region part” showed much significance among cellular components (Fig. 16), which seems to be most influential in the gene expression process thus speculating the fact that they were majorly associated with stress response pathways. The extracellular region serves as the interface between the plant and its environment. It contains receptors, sensors, and other molecules that perceive and transduce environmental signals, including biotic and abiotic stresses. Genes encoding proteins located in the extracellular region are often involved in sensing these signals and initiating signaling cascades that regulate gene expression and physiological responses within the cell.

3.3.7.4 KEGG enrichment analysis

KEGG enrichment analysis identifies the significantly enriched metabolic pathways or signal transduction pathways associated with differentially expressed genes, comparing the whole genome background. the most significant 20 KEGG pathways were selected for display. Higher values correspond to higher significance. Here, plant-pathogen interaction and MAPK signaling pathway in plants showed much significance (Fig.17).

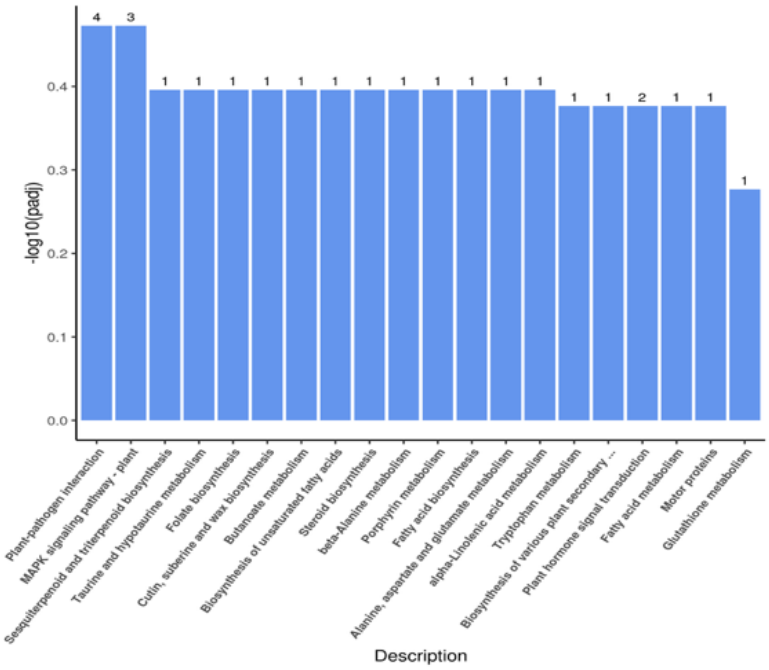

Figure 17. KEGG enrichment analysis of DEGs. Major 20 KEGG pathways are presented here considering their significance in stress response.

KEGG analysis was performed to identify the significantly enriched metabolic pathways. From our data “Plant-pathogen interaction” genes seem to play a diverse role in stress tolerance by coordinating a variety of defense responses, interacting with stress signaling pathways, and modulating physiological processes that improve the plant's capacity to endure both biotic and abiotic stressors. On the other hand, the MAPK signaling pathway enhances stress tolerance by regulating osmotic and ionic balance, redox homeostasis, and stomatal function.

3.3.7.5 Important transcription factor genes in drought stress tolerance:

A coordinated network of transcription factors from different families regulates gene expression in rice plants during drought stress. These transcription factors (TFs) bind to particular DNA sequences in target gene promoters, either activating or inhibiting the expression of the target gene to direct a coordinated stress response. This complex management makes sure the plant can withstand and adapt to the harsh conditions caused by drought. We summarized the occurrence of TF families and protein kinase groups identified among DEGs involved in the drought stress condition of rice plants (Table 8). Transcription factors were listed manually from the gene expression dataset.

TF families	Number	Protein Kinases	Number
ERF (Ethylene Responsive Factor)	31	MAPKKs (Mitogen-Activated Protein Kinase Kinases)	5
NAC (NAM, ATAF1/2 and CUC2)	32		
HSF (Heat Shock Transcription factor)	21	CaMK (Calcium/Calmodulin-Dependent Protein Kinase)	27
bZIP (basic Leucine Zipper)	30		
DREB (Dehydration Responsive Element Binding)	6	SnRK (Sucrose Non-Fermenting 1-Related Kinase)	3
WRKY	28		
MYB (Myeloblastosis)	11		

Table 8. The number of TF families and protein kinase groups identified among DEGs.

Multiple studies illustrated that TF-regulated gene expression and protein kinases play a pivotal role in managing abiotic stress tolerance among various plants. Members of these TF families, extensively involved in the regulation of physiological processes in plants, including abiotic stress responses mostly belong to the DREB (Dehydration Responsive Element Binding), bZIP (basic leucine zipper), AP2/ERF (APETALA2/ethylene-responsive factor), MYB, NAC (NAM, ATAF, and CUC), and WRKY families. Notably, protein kinases like SnRK1, MAPKKs, and CaMK modulate the activity of transcription factors.

To compare gene expression levels within and between samples Ni and GAD4 genome edited (#14-1) in control and drought stress, the FPKM (Fragments Per Kilobase of transcript per Million mapped reads) normalization method was used. This analysis demonstrated that drought stress upregulated several transcripts encoding stress-responsive genes like HSP (heat shock protein), LEA (late embryogenesis abundant) protein, and transcription factors like ERF, MYB, DREB2A, and RAB21 which facilitate the adaptation of the plant to abiotic stresses (Fig. 18).

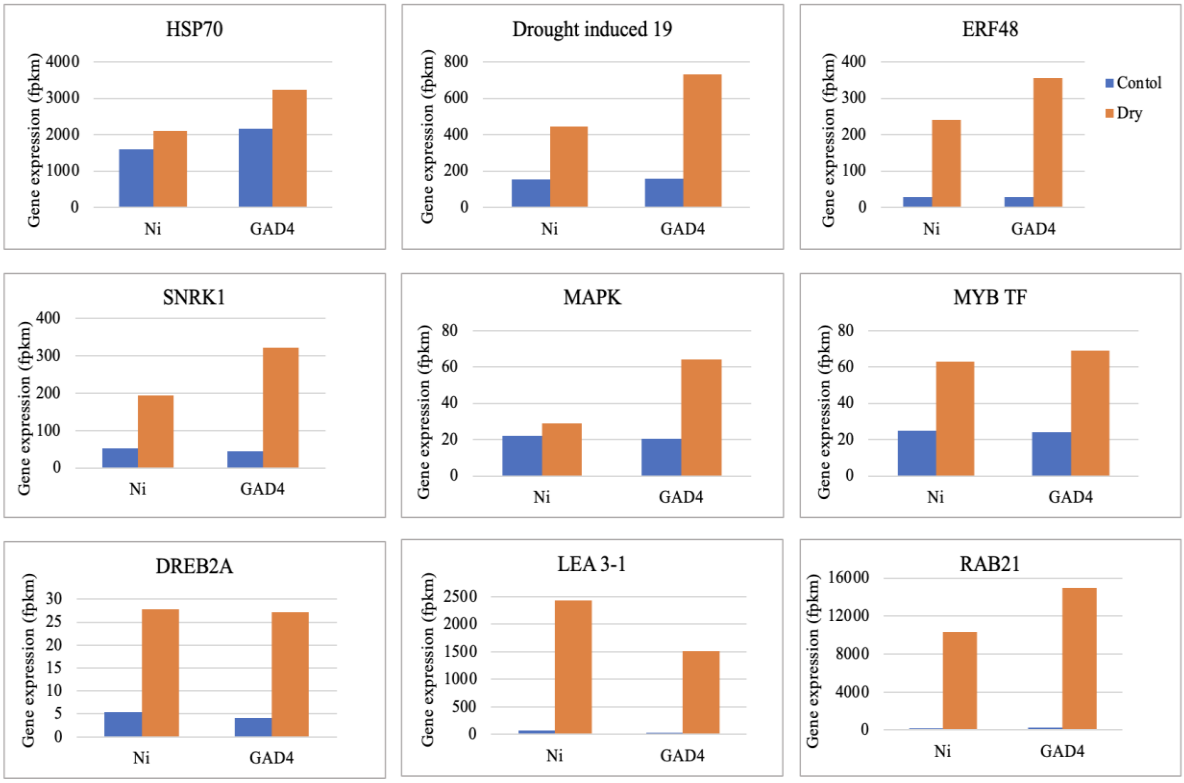

Figure 18. Upregulated genes seem most responsive in drought tolerance. FPKM normalization method showed the upregulated transcript in control and drought conditions. HSP =heat shock protein, ERF= ethylene response factor, SNRK=Sucrose-non fermentation-related protein kinase, MAPK=mitogen-activated protein kinase, DREB= dehydration-responsive element binding protein, LEA =late embryogenesis abundant protein

Moreover, signaling protein kinase such as MAPK (mitogen-activated protein kinase) was found to regulate stress-responsive mechanisms (Sinha et al., 2011). MAPK is a widely studied gene family contributing to plant productivity under changing environmental conditions. Information on contributing genes toward drought stress tolerance, and their networks can impact the potential utilization in crop improvement programs. Taken together, RNA-seq data revealed the intricate and coordinated gene regulation networks that drive biological processes and reactions to stress conditions, resulting in a better understanding of the underlying molecular mechanisms.

3.3.7.6. Validation of RNA-seq data by RT-qPCR analysis

RT-qPCR was performed to validate the results of gene upregulation in RNA-Seq analysis. In this experiment, seedlings of wild-type Ni and C-terminal truncated GAD4 genome edited line #14-1 were treated with drought stress for 24 h. Before and after the stress

treatment, shoot samples were collected for total RNA isolation and further cDNA synthesis as required for RT-qPCR.
We randomly selected several genes to observe the expression pattern. The upregulated gene expression is presented in Figure 19. HSP70, RAB21, and SnRK1 are the notable genes that show the upregulation pattern here.

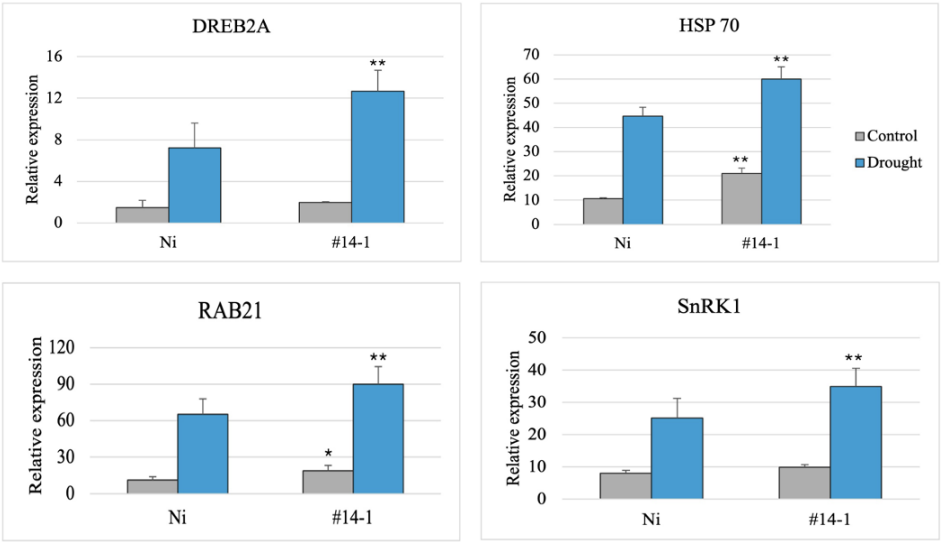

Figure 19. Selected gene upregulation validated by RT-qPCR analysis. TATA-binding protein 2 (TBP2) was used as an internal control. The relative expression level was analyzed using the $2^{-\Delta\Delta CT}$ method. Error bars indicate SD (n=3). Levels of significance were determined by comparing values of wild-type Ni samples to the respective #14-1 samples. Asterisks indicate significant differences (*$P < 0.05$, **$P < 0.01$).

C-terminal truncated genome-edited plants had significantly higher expression levels of heat shock protein 70 (HSP70), responses to ABA proteins (RAB21, a dehydrin gene), and Sucrose-nonfermentation1-related protein kinase1(SnRK1) than wild-type plants under drought stress condition. The DREB2A expression level was seen to be much upregulated in our RT-qPCR analysis. The possible reason might be the sampling bias, though the sampling condition was the same.

Discussion

GABA accumulation is a crucial response in plants subjected to various environmental stresses. When #14-1 seedlings were exposed to 6 h salt stress, their roots showed a 4.3-fold increase in GABA accumulation in comparison to wild-type seedlings under the same stress conditions (Fig. 9a). According to Banerjee et al. (2019), salt stress caused a sharp rise in the endogenous GABA content in the Kalonunia (KN) cultivar (3.7-fold higher than in non-treated lines). This GABA content is crucial for regulating stress tolerance. Increased GABA shunt activity provides an extra carbon source for the TCA cycle to operate in mitochondria, allowing it to avoid salt-sensitive enzymes and aid wheat plants in increasing leaf respiration, hence reducing the effects of salt on plants (Che-Othman et al. 2020). Again, following one hour of treatment, flooding stress increased GABA deposition in the root tissues of GAD4 genome-edited plants (#14-1) by 3.3-fold as compared to wild-type plants (Fig. 9b). These results are consistent with a prior study (Ruperti et al. 2019) that found that when grapevine roots were submerged in water, GABA and other hypoxia-induced metabolites significantly accumulated. In response to hypoxia, activation of the GABA shunt increased GABA levels (António et al. 2016). In the current investigation, we observed a 2.2-fold increase in GABA accumulation in the shoot tissues of line #14-1 following 24-hour drought stress, compared to the wild-type under the same stress circumstances (Fig. 9c). It has been shown in *Arabidopsis* (Mekonnen et al. 2016) that increased GABA accumulation in *gad1/2 x pop2* triple mutants is a drought stress response associated with controlling the stomatal aperture, hence limiting water loss. Increased GABA accumulation after various stressors indicates that GABA functions as a signaling molecule rather than being utilized by the Krebs cycle (Jantaro and Kanwal 2017; Carillo 2018). On the other hand, poor GABA content under stress conditions in mutants with a shorter deletion in the CaMBD coding region (#14–6) most likely results from a combination of decreased enzymatic activity and impaired calmodulin interaction.

As of right now, not enough is known about endogenous GABA-induced gene expression in rice under abiotic stress. After 6 h of salinity stress, our RT-qPCR data demonstrated that the *OsGAD4* gene was elevated in root tissue, reaching 3.2-fold higher expression than the untreated control (Fig. 10a). Surprisingly, the root's *OsGAD4* expression pattern did not match the amount of GABA present at 3 h time point, the mRNA level in the root tissue was falling while the accumulation of GABA was rising. This disparity may be caused by compensatory mechanisms that control the expression of other GAD isoforms, such as *OsGAD1* and/or *OsGAD3*, at that particular salinity level.

When given in combination with exogenous GABA, salt stress dramatically elevated the expression of *SlGAD1-3* in tomato seedling leaves as compared to the control (Wu et al. 2020). When these two treatments were combined, gene expression levels were increased more than when either substance was administered alone. This finding suggested that the transcriptional and metabolic levels of endogenous GABA content were influenced additively by both salt and exogenous GABA. When compared to the untreated control, the first hour of flooding stress caused a nearly 3.1-fold upregulation in mRNA expression in root tissue (Fig.

10b). Among the five GAD isoforms, the highest elevation of *GAD2* was observed in soybeans following flooding stress, and this finding is validated by concurrent augmentation of GABA buildup (Souza et al. 2016). In contrast to untreated samples, drought stress caused dramatic increases in mRNA expression in rice plant shoot tissues, increasing it by 7.5 times at 24 h (Fig. 10c).

Plant cells produce reactive oxygen species (ROS) in response to drought stress. According to reports, ROS produced by stress may have a function in signaling (Hasan et al. 2020). Conversely, *cam5-4* and *cam6-1* mutants (T-DNA insertion of CAM genes) that lack GABA shunt gene expression exhibit a considerable increase in ROS, suggesting that the shunt is important in pathways involved in ROS scavenging (AL-Quraan et al. 2015). CaM may have an indirect effect on the regulation of ROS accumulation through the GABA shunt metabolic pathway and the CaM-regulated GABA production (Bouche et al. 2003). By the process of feedback regulation of several enzymes through CaM modulation, plants may be able to maintain ROS (e.g. H_2O_2) homeostasis (Vridi et al. 2015) and hence offer protection against stress-related damage.

Since the wild-type, genome-edited lines #14-1 and #14-6 share the same promoter region, they showed almost identical expression levels in the current work. However, when exposed to abiotic stressors, line #14-1 showed a considerably higher GABA content. As previously indicated, *Os*GAD4 with the truncated CaMBD seems to exhibit higher enzymatic activity compared to the wild type. This could lead to an increase in the rate at which glutamate is converted to GABA and an increase in the amount of GABA in tissues that are exposed to abiotic stressors.

The salinity, flooding, and drought stress tolerance in *OsGAD4* genome-edited plants were investigated. #14-1 line showed significantly higher survival rates (44.2%, 59.6%, and 34.5%, respectively) compared with wild-type controls (17.3%, 25.6%, and 12.2%, respectively) but #14-6 was marked to be like wild type (Fig. 10, Table 7). GABA-enriched plants' defense function to reduce stress damage was correlated with a trend towards lesser biomass loss in #14-1 plants (Table 2). The enhanced resistance to cold, high salt and drought displayed by transgenic rice plants overexpressing the *OsDREB1A* and *OsDREB1B* genes probably helped explain the higher survival rate of these plants under these circumstances (Ito et al. 2006). Our findings suggest that the critical role of GABA in the defense system along with those of other signaling molecules and plant growth regulators, may affect a plant's ability to withstand abiotic stress.

The current study revealed that the genetically modified *OsGAD4* gene induces abiotic stress tolerance in rice seedlings in the early vegetative stage. Similarly, transgenic rice plants that overexpress the ethylene response factor [ERF] family members AP57 and AP59 offer resistance to extreme salt and drought (Oh et al. 2009). Furthermore, Campo et al. (2014) demonstrated that *OsCPK4* expression confers plant tolerance to a variety of stress conditions, raising the prospect that this gene, which codes for a crucial protein in the stress response system, can offer enough tolerance to multiple stresses. Notably, high endogenous GABA

actively modulates the stress resistance mechanism in rice seedlings, as demonstrated by the C-terminally truncated mutant of *OsGAD1, OsGAD3*, and their hybrid line, which also demonstrated strong tolerance to abiotic stresses to varying degrees (unpublished data). Taken together, higher expression of GABA-shunt genes and activation of antioxidant enzymes, which have been described as increased GABA-induced counteracting mechanisms in previous research, may be responsible for superior stress tolerance in OsGAD4 genome-edited plants (Kumar et al. 2017; Wang et al. 2017). Thus, it is tempting to draw a connection between strong GABA production in the vegetative tissues of rice plants and stress tolerance. To the best of our knowledge, this is the first work assessing how endogenous GABA regulates the rice *GAD* gene's response to abiotic stress. Other crop plants could benefit from this method of altering putative GAD by deleting CaMBD by genome editing, which would increase GABA buildup and improve abiotic stress resistance.

Due to metabolic imbalance during stress results in increased ROS production thus causing oxidative stress. ROS can include singlet oxygen ($^1O_2$), superoxide radicals ($O_2^{\cdot-}$), hydrogen peroxide (H_2O_2), and radical hydroxyls ($OH^{\cdot}$) (Gupta and Huang 2014). If the ROS accumulation is increasing in the cells continuously, that can cause severe oxidative damage to membranes. Various ROS-detoxifying proteins can mitigate this damage, i.e., CAT, POD, APX, etc. In the current study, the abovementioned antioxidant enzyme activity was significantly higher in #14-1 leaf tissues under multiple stress conditions (Fig.12). According to Mishra et al. (2013), rice plants' salt tolerance is attributed to high levels of non-enzymatic antioxidants and antioxidant enzymes during stress. Maintaining strong antioxidant enzymatic activity to scavenge ROS has been related to greater plant tolerance to various environmental stressors (Mishra et al. 2013). The enhanced antioxidant enzyme activity in the study might be a mechanism to decrease or avoid oxidative damage and increase plant stress resilience. Moreover, DAB staining supports the ROS accumulation trend in response to different abiotic stresses (Fig. 13). Leaf phenotypes after DAB staining of #14-1 demonstrated that less H_2O_2 accumulated in *Os*GAD4- C-terminal truncated mutants than in wild-type and #14-6 after drought stress. These results suggest high GABA content positively regulates abiotic stress tolerance particularly salt and drought tolerance by curbing ROS accumulation.

RNA seq analysis reveals the differentially expressed genes and their upregulation and downregulation. Up-regulation of genes refers to an increase in the expression of certain genes. A large number of up-regulated genes indicate that the organism is activating it to react to internal or external stimuli or to adapt to its environment. Many stress-responsive genes are downregulated as part of this regulatory response. These downregulated genes may include those involved in growth and development processes that are temporarily inhibited during stress to conserve energy and resources. Additionally, genes involved in unnecessary metabolic pathways may be downregulated to prioritize resources for stress tolerance mechanisms. Stress conditions can trigger the activation of transcriptional repressors or chromatin-modifying enzymes that can actively suppress or alter the expression of specific genes (Smith and workman, 2012).

Moreover, gene ontology suggests that “extracellular space” and “extracellular region part” are the most responsive pathways in cellular components influencing gene expression. Extracellular proteins contribute to the structural integrity and stability of tissues and organs, including the cell wall, extracellular matrix, and cuticle. These proteins possibly provide mechanical support, adhesion, and elasticity to withstand environmental stresses, such as drought. Changes in the expression of genes encoding extracellular structural proteins can affect tissue architecture, barrier function, and stress tolerance in plants.

HSP70, RAB21, SnRK1, and MAPK are notable among the upregulated genes specifically responsive to stress tolerance mechanism in the current study (Fig.18). Various studies previously reported the involvement of these genes in stress tolerance mechanism. Heat shock protein 70 (HSP70) proteins play a crucial role in mitigating the detrimental effects of abiotic stresses in plants (Ahmad et al. 2022), whereas ERF48 was found to enhance root growth and drought tolerance in rice (Jung et al. 2017). Moreover, SnRK1 was stated to modulate specific stress-inducible genes in rice and *Arabidopsis* involved in physiological adaptation to stress conditions (Cho et al. 2012). MAPK cascades participate in responses to environmental stresses by regulating the expression of linked genes and plant hormone synthesis (Lin et al. 2021). MAPKs are important tools that regulate growth and development, cell division, proliferation, apoptosis, hormonal response, and other stress responses in plant species. Besides, we confirmed the gene upregulation pattern of important genes like Dehydration Responsive Element Binding Protein (DREB2A), HSP70, SnRK1 and RAB21 through RT-qPCR analysis (Fig. 19). Previous study revealed that the expression of OsDREB2A was induced by drought stress (Dubouzet et al. 2003). Moreover, a drought-responsive gene, RAB21, was constitutively expressed in drought stress (Lee et al. 2018).

Drought stress can impose a subtle or abrupt effect on plant cells depending on the severity of the stress. It has both broad and specific impacts on plant growth and development. Thus, plant responses to drought stress are dynamic, including numerous stress detection and signal transduction pathways. GABA plays a strongly positive role in conferring plant tolerance to stress. The up-regulation of the aforementioned stress-protective genes and transcriptional factors could contribute to improved drought tolerance in rice plants.

Chapter IV
General Conclusion

4.1 Truncated mutant of *Os*GAD4 generated by genome editing, yielded significantly higher GABA in rice grain

In our study, C-terminal truncation of the coding region of *OsGAD4* was performed successfully by genome editing using CRISPR/Cas9. The genome-edited rice line (#14-1) produced almost 9-fold higher GABA content than wild-type Ni. As a powerful tool, genome editing technique allows targeted modifications at specific genomic locations for crop improvement; though the transgenic method offers much more choices to consider by integrating genes of interest under strong constitutive or inducible promoters. Precise control over the expression of target genes in a variety of tissues is possible with transgenic overexpression which would be quite difficult in the genome editing approach. For instance, GABA-fortified rice was developed through a transgenic method yielding almost 60-fold GABA in comparison to the wild type (Kowaka et al. 2015) whereas, in genome editing, GABA increment remained under 10-fold. However, the potential application of the current study could outweigh the constraints by the production and consumption of GABA-enriched rice for conscious consumers because of its potential health benefits.

4.2 GABA-enriched mutant showed enhanced tolerance level against multiple stress conditions compared to wild-type

Multiple abiotic stress conditions (salinity, flooding, drought) promoted the accumulation of GABA in vegetative tissues of the truncated version of *Os*GAD4 mutant (#14-1). Expression levels of *OsGAD4* were upregulated when subjected to abiotic stresses and expression levels were consistent with the GABA accumulation trend in stress conditions. Additionally, it is obvious that the survival rates of the truncated version of *OsGAD4* genome-edited rice plants were significantly higher than that of control plants, suggesting the stress tolerance induction of *OsGAD4*. Besides, mutants with small deletion at the C-terminal region of CaMBD (#14-6) resulting in longer polypeptide chain neither produce significant GABA nor considerable stress tolerance response. The mutant's lower GABA concentration may interfere with stress signaling pathways and metabolites, making it more difficult for the plant to withstand stress conditions. A strong positive correlation between high antioxidant enzyme activity and low ROS accumulation suggests effective ROS scavenging and stress tolerance in the #14-1 line. On the other hand, genome editing can shorten the time needed to create new rice genotypes that are more resilient to abiotic stresses, and it has immense prospects to ensure sustainable food security in areas vulnerable to climate-related adversities. This report opens a new horizon to gain insight into endogenous GABA-mediated abiotic stress tolerance in plants.

4.3 RNA-seq analysis sheds light on the molecular mechanisms underlying plant stress responses

RNA-seq analysis reveals a higher number of uniquely expressed genes in the #14-1 line compared to the wild-type which might have a major role in drought stress tolerance. The gene networks included transcripts coding for water stress-related protein, drought stress-induced protein, heat stress transcription factors and so on. Most of these transcripts have been found to be involved in drought stress tolerance. Among these, HSPs (Heat Shock Proteins) have key roles in acting as molecular chaperones and antioxidants against abiotic stresses. HSPs have been reported to enhance abiotic stress tolerance in rice, particularly in drought (Xiang et al. 2018). The transcripts coding for transcription factors like MYB, ERF, SNRK, and MAPK were also identified amongst the drought up-regulated transcripts. These are known as regulators of the stress-responsive gene expression in plants.

Stress-responsive pathways are comprised of different categories. The key genes mainly code for proteins that have either metabolic or regulatory roles, such as involvement in detoxification, biosynthesis of osmolytes, proteolysis of cellular substrates, and many more. The other category involved in the regulatory process mainly includes transcription factors (TFs) and signaling protein kinases specifically coordinate signal transduction and gene expression during stress responses (Wani et al. 2014). In the current study, cellular components are the major influencer group of drought stress tolerance mechanism specifically by regulating MAPK signaling pathway and plant hormone signal transduction. Upregulation of the drought stress-responsive gene expression helps us to understand coordinated and comprehensive stress response. To sum up, these data suggest that endogenous GABA increased drought tolerance via modulating gene expression and related stress signaling and protection mechanisms. Such findings have valuable implications for plant physiology as well as molecular studies under multiple abiotic stresses.

4.4 Our hypothesis on GABA-mediated abiotic stress tolerance

Abiotic stress response in rice plants primarily enhanced GABA accumulation in vegetative tissues. involves the regulation of metabolites, reactive oxygen species (ROS) accumulation, and cell wall damage. ROS may react with proteins, lipids, and DNA, causing oxidative damage and impairing normal cell function. However, GABA promotes ROS detoxification in plants, which is accomplished by triggering antioxidative defense mechanisms (Fig. 20).

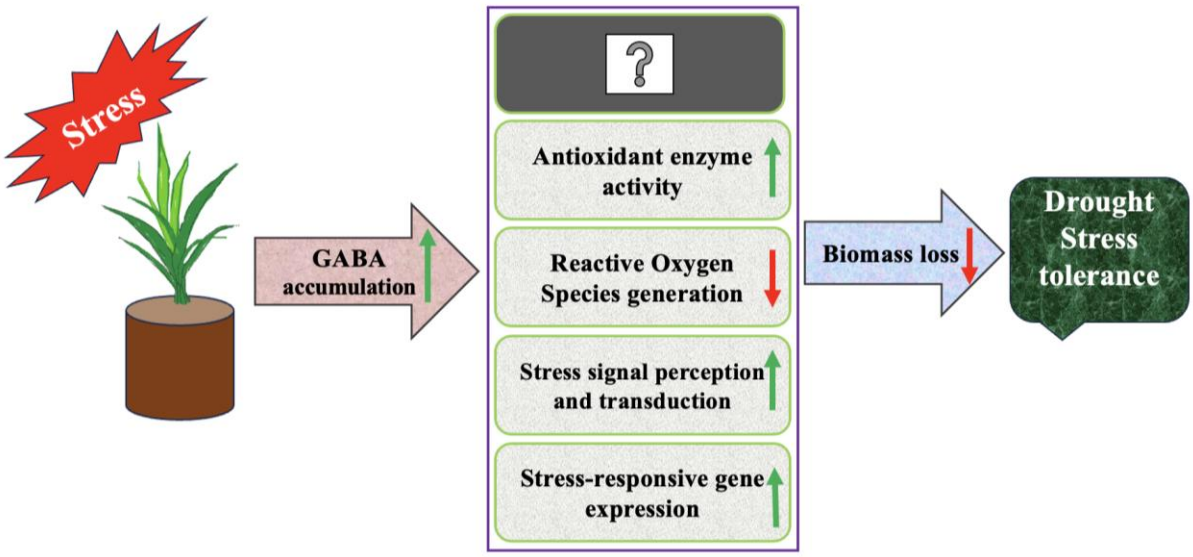

Figure 20. Simplified diagram based on our hypothesis of drought stress tolerance modulated by GABA.

Upon exposure to abiotic stresses, tolerant cells activate their stress signal perception and transduction pathways which results in the upregulation of stress-responsive genes and thus protecting the cell through retention of its biomass. However, in this stress regulatory mechanism, there could be some vital elements that are unexplored yet in this study. They might have some important role as protective metabolite, protein or transcription factor positively regulating the stress tolerance in relation to GABA enrichment. Further research is required to reveal that.

References

Abdel Razik ES, Alharbi BM, Pirzadah TB, Alnusairi GS, Soliman MH, Hakeem KR (2021) γ-Aminobutyric acid (GABA) mitigates drought and heat stress in sunflower (*Helianthus annuus* L.) by regulating its physiological, biochemical and molecular pathways. Physiol Plant 172(2):505–527. https://doi.org/10.1111/ppl.13216

Ahmad MZ, Shah Z, Ullah A, Ahmed S, Ahmad B, Khan A (2022) Genome wide and evolutionary analysis of heat shock protein 70 proteins in tomato and their role in response to heat and drought stress. Mol Biol Rep 49(12):11229-11241. https://doi.org/10.1007/s11033-022-07734-1

Akama K, Akihiro T, Kitagawa M, Takaiwa F (2001) Rice (*Oryza sativa*) contains a novel isoform of glutamate decarboxylase that lacks an authentic calmodulin-binding domain at the C-terminus. Biochim Biophys Acta 1522:143–150. https://doi.org/10.1016/s0167-4781(01)00324-4

Akama K and Takaiwa F (2007) C-terminal extension of rice glutamate decarboxylase (*OsGAD2*) functions as an autoinhibitory domain and overexpression of a truncated mutant results in the accumulation of extremely high levels of GABA in plant cells. J Exp Bot 58:2699–2707. https://doi.org/10.1093/jxb/erm120

Akama K, Kanetou J, Shimosaki S, Kawakami K, Tsuchikura S, Takaiwa F (2009) Seed-specific expression of truncated OsGAD2 produces GABA-enriched rice grains that influence a decrease in blood pressure in spontaneously hypertensive rats. Transgenic Res 18:865–876. https://doi.org/10.1007/s11248-009-9272-1

Akama K, Akter N, Endo H, Kanesaki M, Endo M, Toki S (2020) An *In Vivo* Targeted Deletion of the Calmodulin-Binding Domain from Rice Glutamate Decarboxylase 3 (*OsGAD3*) Increases γ-Aminobutyric Acid Content in Grains. Rice 13:20. https://doi.org/10.1186/s12284-020-00380-w

Akihiro T, Koike S, Tani R, Tominaga T, Watanabe S, Iijima Y, Aoki K, Shibata D, Ashihara H, Matsukura C, Akama K, Fujimura T, Ezura H (2008) Biochemical mechanism on GABA accumulation during fruit development in tomato. Plant Cell Physiol 49:1378–1389. https://doi.org/10.1093/pcp/pcn113

AL-Quraan NA (2015) GABA shunt deficiencies and accumulation of reactive oxygen species under UV treatments: insight from *Arabidopsis thaliana* calmodulin mutants. Acta Physiol Plant 37:86. https://doi.org/10.1007/s11738-015-1836-5

António C, Päpke C, Rocha M, Diab H, Limami AM, Obata T et al. (2016) Regulation of primary metabolism in response to low oxygen availability as revealed by carbon and nitrogen isotope redistribution. Plant Physiol 170: 43–56. https://doi.org/10.1104/pp.15.00266

Arazi T, Baum G, Snedden WA, Shelp BJ, Fromm H (1995) Molecular and biochemical analysis of calmodulin interactions with the calmodulin binding domain of plant glutamate decarboxylase. Plant Physiol 108: 551–561. https://doi.org/10.1104/pp.108.2.551

Azevedo RA, Alas RM, Smith RJ, Lea PJ (1998) Responses of antioxidant enzymes to transfer from elevated carbon dioxide to air and ozone fumigation, in the leaves and roots of wild type and catalase-deficient mutant of barley. Physiol Plant 104:280–292

Bai TH, Li CY, Ma FW, Shu HR, Han MY (2009) Exogenous salicylic acid alleviates growth inhibition and oxidative stress induced by hypoxia stress in *Malus robusta* Rehd. J Plant Growth Regul 28:358–366

Banerjee A, Ghosh P, Roychoudhury A (2019) Salt acclimation differentially regulates the metabolites commonly involved in stress tolerance and aroma synthesis in indica rice cultivars. Plant Growth Regul 88:87–97. https://doi.org/10.1007/s10725-019-00490-6

Bao H, Chen X, Lv S, Jiang P, Feng J, Fan P, Nie L, Li Y (2015) Virus induced gene silencing reveals control of reactive oxygen species accumulation and salt tolerance in tomato by γ-aminobutyric acid metabolic pathway. Plant Cell Environ 38:600–613 https://doi.org/10.1111/pce.12419

Baum G, Chen Y, Arazi T, Takatsuji H, Fromm H (1993) A plant glutamate decarboxylase containing a calmodulin binding domain. Cloning, sequence, and functional analysis. J Biol Chem 268:19610–19617

Baum G , Lev-Yadun S, Fridmann Y, Arazi T, Katsnelson H, Zik M, Fromm H (1996) Calmodulin binding to glutamate decarboxylase is required for regulation of glutamate and GABA metabolism and normal development in plants. EMBO J 15:2988–2996

Bouche N, Fait A, Bouchez D, Moller SG, Fromm H (2003). Mitochondrial succinic-semialdehyde dehydrogenase of the gamma-aminobutyrate shunt is required to restrict levels of reactive oxygen intermediates in plants. Proc Natl Acad Sci USA 100:6843–6848. https://doi.org/10.1073/pnas.1037532100

Bown AW and Shelp BJ (1997) The metabolism and functions of γ-aminobutyric acid. Plant Physiol 115:1–5. https://doi.org/10.1104/pp.115.1.1

Campo S, Baldrich P, Messeguer J, Lalanne E, Coca M, Segundo BS (2014) Overexpression of a Calcium-Dependent Protein Kinase Confers Salt and Drought Tolerance in Rice by Preventing Membrane Lipid Peroxidation. Plant Physiol 165(2):688–704. https://doi.org/10.1104/pp.113.230268

Carillo P (2018) GABA shunt in durum wheat. Front Plant Sci 9:100. https://doi.org/10.3389/fpls.2018.00100

Chen K and Gao C (2013) Targeted genome modification technologies and their applications in crop improvements. Plant Cell Rep 33:575–83. https://doi.org/10.1007/s00299-013-1539-6

Chen S, Zhang N, Zhou G, Hussain S, Ahmed S, Tian H, Wang S (2021) Knockout of the entire family of AITR genes in *Arabidopsis* leads to enhanced drought and salinity tolerance without fitness costs. BMC Plant Biol 21:137. https://doi.org/10.1186/s12870-021-02907-9

Che-Othman MH, Jacoby RP, Millar AH, Taylor NL (2020) Wheat mitochondrial respiration shifts from the tricarboxylic acid cycle to the GABA shunt under salt stress. New Phytol 225:1166–1180. https://doi.org/10.1111/nph.15713

Cho YH, Hong JW, Kim EC, Yoo SD (2012) Regulatory functions of SnRK1 in stress-responsive gene expression and in plant growth and development. Plant Physiol. 158(4):1955-64. https://doi.org/10.1104/pp.111.189829.

Cong L, Ran FA, Cox D, Lin S, Barretto R, Habib N, Hsu PD, Wu X, Jiang W, Marraffini L (2013) Multiplex genome engineering using CRISPR/Cas systems. Science 339:819–823. https://doi.org/ 10.1126/science.1231143

Curtis DR and Johston GAR (1974) Amino acids transmitters in the mammalian central nervous system. Ergeb Physiol 69:97–188

Diana M, Quílez J, Rafecas M (2014) Gamma-aminobutyric acid as a bioactive compound in foods: a review. J Funct Foods 10:407–420. https://doi.org/10.1016/j.jff.2014.07.004

Dubouzet JG, Sakuma Y, Ito Y, Kasuga M, Dubouzet EG, Miura S, Seki M, Shinozaki K, Yamaguchi-Shinozaki K (2003) *OsDREB* genes in rice, *Oryza sativa* L., encode transcription activators that function in drought, high-salt, and cold-responsive gene expression, The Plant J, 33:751-763.

Fait A, Fromm H, Walter D, Galili G, Fernie AR (2008) Highway or byway: The metabolic role of the GABA shunt in plants. Trends Plant Sci 13:14–19. https://doi.org/ 10.1016/j.tplants.2007.10.005

Food and Agriculture Organization (FAO). (openknowledge.fao.org) Food Outlook, June 2022; Food and Agriculture Organization (FAO): Rome, Italy.

Fukagawa NK, Ziska LH (2019) Rice: Importance for Global Nutrition. J Nutr Sci Vitaminol (Tokyo).;65(Supplement): S2-S3. https://doi.org/10.3177/jnsv.65.S2.

Gao C (2015) Genome editing in crops: from bench to field. Natl Sci Rev 2:13–5. https://doi.org/10.1093/nsr/nwu054

Gottesmann C (2002) GABA mechanisms and sleep. Neuroscience 111:231–239. https://doi.org/0.1016/s0306-4522(02)00034-9

Gupta B and Huang B (2014) Mechanism of salinity tolerance in plants: physiological, biochemical, and molecular characterization. Int J Genomics 701596:18. https://doi.org/10.1155/2014/701596

Gut H, Dominici P, Pilati S, Astegno A, Petoukhov MV, Svergun DI, Grütter MG, Capitani G (2009) A common structural basis for pH- and calmodulin-mediated regulation in plant glutamate decarboxylase. J Mol Biol 392:334–351. https://doi.org/10.1016/j.jmb.2009.06.080

Hasan MM, Alharby HF, Uddin MN, Ali MA, Anwar Y, Fang XW, Hakeem KR, Alzahrani Y, Hajar AS (2020) Magnetized water confers drought stress tolerance in *Moringa* biotype via modulation of growth, gas exchange, lipid peroxidation and antioxidant activity. Pol J Environ Stud 29:1625–1636. https://doi.org/10.15244/pjoes/110347

Hasan MM, Alabdallah NM, Alharbi BM, Waseem M, Yao G, Liu XD, Abd El-Gawad HG, El-Yazied AA, Ibrahim MF, Jahan MS, Fang XW (2021) GABA: A key player in drought stress resistance in plants. Int J Mol Sci 22(18), 10136. https://doi.org/ 0.3390/ijms221810136

Hood EE, Gelvin SB, Melchers LS, Hoekema A (1993) New *Agrobacterium* helper plasmids for gene transfer to plants. Transgenic Res 2:208–218

Huber R, Kondo D, Shi X, Prescot A, Clark E, Renshaw PF, Yurgelun-Todd DA (2018) Relationship of executive functioning deficits to N-acetyl aspartate. (NAA) and gamma-aminobutyric acid (GABA) in youth with bipolar disorder. J Affect Disord. 225:71–8. https://doi.org/10.1016/j.jad.2017.07.052

Intergovernmental Panel on Climate Change (IPCC). Climate Change 2022: Impacts, Adaptation, and Vulnerability; Intergovernmental Panel on Climate Change (IPCC): Geneva, Switzerland.

Ito Y, Katsura K, Maruyama K, Taji T, Kobayashi M, Seki M, Shinozaki K, Yamaguchi-Shinozaki K (2006) Functional analysis of rice DREB1/CBF-type transcription factors involved in cold-responsive gene expression in transgenic rice. Plant Cell Physiol 47(1):141-53. https://doi.org/10.1093/pcp/pci230

Jantaro S, Kanwal S (2017) Low-Molecular-Weight Nitrogenous Compounds (GABA and Polyamines) in Blue-Green Algae. Algal Green Chemistry. https://doi.org/10.1016/B978-0-444-63784-0.00008-4

Ji J, Shi Z, Xie T, Zhang X, Chen W, Du C, Sun J, Yue J, Zhao X, Jiang Z (2020) Responses of GABA shunt coupled with carbon and nitrogen metabolism in poplar under NaCl and CdCl2 stresses. Ecotox Environ Saf 193:110322. https://doi.org/ 10.1016/j.ecoenv.2020.110322

Jie F, Yin G, Yang W, Yang M, Gao S, Lv J, Li B (2018) Stress in regulation of GABA amygdala system and relevance to neuropsychiatric diseases. Front Neurosci 12:562. https://doi.org/ 10.3389/fnins.2018.00562

Jinek M, Chylinski K, Fonfara I, Hauer M, Doudna JA, Charpentier E (2012) A programmable dual-RNA–guided DNA endonuclease in adaptive bacterial immunity. Science 337:816–821. https://doi.org/ 10.1126/science.1225829

Jung H, Chung PJ, Park SH, Redillas MCFR, Kim YS, Suh JW, Kim JK (2017) Overexpression of OsERF48 causes regulation of OsCML16, a calmodulin-like protein gene that enhances root growth and drought tolerance. Plant Biotechnol J 15(10):1295-1308. https://doi.org/10.1111/pbi.12716.

Kanehisa M, Goto S (2000) KEGG: kyoto encyclopedia of genes and genomes. Nucleic acids research 28(1): 27-30. https://doi.org/10.1093/nar/28.1.27

Kawahara Y, Oono Y, Wakimoto H, Ogata J, Kanamori H, Sasaki H, Mori S, Matsumoto T, Itoh T (2016) TENOR: Database for Comprehensive mRNA-Seq Experiments in Rice. Plant Cell Physiol 57 (1) e7:1-13. https://doi.org/10.1093/pcp/pcv179

Kinnersley AM and Turano FJ (2000) Gamma aminobutyric Acid (GABA) and plant responses to stress. Cri Rev Plant Sci 19:479–509

Kisaka H, Kida T, Miwa T (2006) Antisense suppression of glutamate decarboxylase in tomato (*Lycopersicon esculentum* L.) results in accumulation of glutamate in transgenic tomato fruits. Plant Biotechnol 23:267–274. https://doi.org/10.5511/plantbiotechnology.23.267

Koike S, Matsukura C, Takayama M, Asamizu E, Ezura H (2013) Suppression of γ - aminobutyric acid (GABA) transaminases induces prominent GABA accumulation, dwarfism and infertility in the tomato (*Solanum lycopersicum* L.). Plant Cell Physiol 54:793–807.

Komatsuzaki N, Tsukahara K, Toyoshima H, Suzuki T, Shimizu N, Kimura T (2007) Effect of soaking and gaseous treatment on GABA content in germinated brown rice. J Food Eng 78:556-560. https://doi.org/10.1016/j.jfoodeng.2005.10.036

Kowaka E, Shimajiri Y, Kawakami K, Tongu M, Akama K (2015) Field trial of GABA fortified rice plants and oral administration of milled rice in spontaneously

hypertensive rats. Transgenic Res 24:561–569. https://doi.org/10.1007/s11248-014-9859-z

Kumar N, Dubey AK, Upadhyay AK, Gautam A, Ranjan R, Srikishna S, Sahu N, Behera SK, Mallik S (2017) GABA accretion reduces Lsi-1 and Lsi-2 gene expressions and modulates physiological responses in *Oryza sativa* to provide tolerance towards arsenic. Sci Rep 7:8786. https://doi.org/10.1038/s41598-017-09428-2

Kumar VVS, Verma RK, Yadav SK, Yadav P, Watts A, Rao MV, Chinnusamy V (2020). CRISPR-Cas9 mediated genome editing of drought and salt tolerance (*OsDST*) gene in indica mega rice cultivar MTU1010. Physiol Mol Biol Plants 26:1099–1110. https://doi.org/10.1007/s12298-020-00819-w

Lee H, Cha J, Choi C, Choi N, Ji HS, Park SR, Lee S, Hwang DJ (2018). Rice WRKY11 plays a role in pathogen defense and drought tolerance. Rice (N Y) 11 (1), 5. https://doi.org/10.1186/s12284-018-0199-0

Lei Y, Lu L, Liu HY, Li S, Xing F, Chen LL (2014) CRISPR-P: a web tool for synthetic single-guide RNA design of CRISPR-system in plants. Mol Plant 7:1494–1496. https://doi.org/10.1093/mp/ssu044

Li L, Dou N, Zhang H, Wu C (2021) The versatile GABA in plants. Plant Signal Behav 16:3. https://doi.org/10.1080/15592324.2020.1862565

Li P, Li X, Jiang M (2021) CRISPR/Cas9-mediated mutagenesis of WRKY3 and WRKY4 function decreases salt and Me-JA stress tolerance in *Arabidopsis Thaliana.* Mol Biol Rep 48. https://doi.org/10.1007/s11033-021-06541-4

Liao Y, Smyth GK, Shi W (2014) featureCounts: an efficient general purpose 5 program for assigning sequence reads to genomic features. Bioinformatics 30(7):923-30. https://doi.org/10.1093/bioinformatics/btt656

Lin L, Wu J, Jiang M, Wang Y (2021) Plant Mitogen-Activated Protein Kinase Cascades in Environmental Stresses. Int J Mol Sci 3;22(4):1543. https://doi.org/10.3390/ijms22041543.

Liu H, Hu M, Wang Q, Cheng L, Zhang Z (2018) Role of papain-like cysteine proteases in plant development. Front Plant Sci 871. https://doi.org/10.3389/fpls.2018.01717

Liu JX, Gao YL, Xu Y, Zheng CH, You J (2014) Differential Expression Analysis on RNA-Seq Count Data Based on Penalized Matrix Decomposition. IEEE Transactions on NanoBioscience 13,1:12-18. https://doi.org/10.1109/TNB.2013.2296978

Liu L, Zhang J, Xu J, Li Y, Guo L, Wang Z, Zhang X, Zhao B, Guo YD, Zhang N (2020) CRISPR/Cas9 targeted mutagenesis of SlLBD40, a lateral organ boundaries domain

transcription factor, enhances drought tolerance in tomato. Plant Sci 301:110683. https://doi.org/10.1016/j.plantsci.2020.110683

Liu LL, Zhai HQ, Wan J-M (2005) Accumulation of γ-Aminobutyric acid in Giant- embryo Rice grain in relation to glutamate decarboxylase activity and its gene expression during water soaking. Cereal Chem 82:191–196. https://doi.org/10.1094/CC-82-0191

Livak KJ, Schmittgen TD (2001) Analysis of relative gene expression data using real-time quantitative PCR and the 2(-Delta Delta C(T)) Method. Methods 25(4):402–408. https://doi.org/10.1006/ meth.2001.1262

Mei X, Chen Y, Zhang L, Fu X, Wei Q, Grierson D, Zhou Y, Huang Y, Dong F, Yang Z (2016) Dual mechanisms regulating glutamate decarboxylases and accumulation of gamma-aminobutyric acid in tea (*Camellia sinensis*) leaves exposed to multiple stresses. Sci Rep 6:23685. https://doi.org/10.1038/srep23685

Mekonnen DW, Flügge U-I, Ludewig F (2016) Gamma-aminobutyric acid depletion affects stomata closure and drought tolerance of *Arabidopsis thaliana*. Plant Sci 245:25–34. https://doi.org/10.1016/j.plantsci.2016.01.005

Mikami M, Toki S, Endo M (2015) Comparison of CRISPR/Cas9 expression constructs for efficient targeted mutagenesis in rice. Plant Mol Biol 88:561– 572. https://doi.org/10.1007/s11103-015-0342-x

Miladinovic D, Antunes D, Yildirim K, Bakhsh A, Cvejić S, Kondić-Špika A, Jeromela AM, Opsahl-Sorteberg HG, Zambounis A, Hilioti Z (2021) Targeted plant improvement through genome editing: from laboratory to field. Plant Cell Rep 40:935-951. https://doi.org/10.1007/s00299-020-02655-4

Mishra P, Bhoomika K, Dubey RS (2013) Differential responses of antioxidative defense system to prolonged salinity stress in salt-tolerant and salt-sensitive Indica rice (*Oryza sativa* L.) seedlings. Protoplasma 250:3–19. https://doi.org/10.1007/s00709-011-0365-3

Mortazavi A, Williams B A, McCue K, Schaeffer L, Wold B (2008) Mapping and quantifying mammalian transcriptomes by RNA-Seq. Nat Methods 5(7): 621-628. https://doi.org/10.1038/nmeth.1226

Murashige T and Skoog F (1962) A revised medium for rapid growth and bio assays with tobacco tissue cultures. Physiol Plantarum 15:473–497

Murray MG and Thompson WF (1980) Rapid isolation of high molecular weight plant DNA. Nucleic Acids Res 8:4321–4325. https://doi.org/10.1093/nar/8.19.4321

Nakano Y, Asada K (1981) Hydrogen peroxide is scavenged by ascobate-specific peroxidase in spinach chloroplasts. Plant Cell Physiol 22:867–880

Nemeroff CB (2003) The role of GABA in the pathophysiology and treatment of anxiety disorders. Psychopharmacol Bull 37:133–146.

Nonaka S, Arai C, Takayama M, Matsukura C, Ezura H (2017) Efficient increase of ɣ-aminobutyric acid (GABA) content in tomato fruits by targeted mutagenesis. Sci Rep 7:7057. https://doi.org/10.1038/s41598-017-06400-y

Oh SJ, Kim YS, Kwon, CW, Park HK, Jeong JS, Kim JK (2009) Overexpression of the transcription factor AP37 in rice improves grain yield under drought conditions. Plant Physiol 150(3):1368–1379. https://doi.org/10.1104/pp.109.137554

Ohtsubo K, Suzuki K, Yasui Y, Kasumi T (2005) Bio-functional components in the processed pre-germinated brown rice by a twin-screw extruder. J Food Comp Ana 18:303-316. https://doi.org/10.1016/j.jfca.2004.10.003

Ozawa K (2009) Establishment of a high efficiency *Agrobacterium*-mediated transformation system of rice (*Oryza sativa* L.). Plant Sci 176(4):522-7. https://doi.org/10.1016/j.plantsci.2009.01.013

Panda D, Mishra SS, Behera PK (2021) Drought Tolerance in Rice: Focus on Recent Mechanisms and Approaches. Rice Sci 28:119–132. https://doi.org/10.1016/j.rsci.2021.01.002.

Park KB and Oh SH (2007) Production of yogurt with enhanced levels of gamma-aminobutyric acid and valuable nutrients using lactic acid bacteria and germinated soybean extract. Bioresour Technol 98:1675–1679. https://doi.org/10.1016/j.biortech.2006.06.00

Rashmi D, Zanan R, John S, Khandagale K, Nadaf A (2018) Chapter 13 - γ-aminobutyric acid (GABA): biosynthesis, role, commercial production, and applications. Stud Nat Products Chem 57:413–452.

Renault H, Amrani AE, Palanivelu R, Updegraff EP, Yu A, Renou J, Preuss D, Bouchereau A, Deleu C (2011) GABA accumulation causes cell elongation defects and a decrease in expression of genes encoding secreted and cell-wall-related proteins in *Arabidopsis thaliana*. Plant Cell Physiol 52:894–908. https://doi.org/ 10.1093/pcp/pcr041

Riyazuddin R, Nisha N, Singh K, Verma R, Gupta R (2021). Involvement of dehydrin proteins in mitigating the negative effects of drought stress in plants. Plant Cell Rep, 41 (3), 519–533. https://doi.org/ 10.1007/s00299-021-02720-6

Ruperti B, Botton A, Populin F, Eccher G, Brilli M, Quaggiotti S, Trevisan S, Cainelli N, Guarracino P, Schievano E, Meggio F (2019) Flooding responses on grapevine: a physiological, transcriptional, and metabolic perspective. Front Plant Sci 10:339. https://doi.org/10.3389/fpls.2019.00339.

Saikusa T, Horino T, Mori Y (1994) Distribution of free amino acids in the rice kernel and kernel fractions and the effect of water soaking on the distribution. J Agr Food Chem 42:1122-1125

Salah A, Zhan M, Cao C, Han Y, Ling L, Liu Z, Li P, Ye M, Jiang Y (2019) γ-Aminobutyric acid promotes chloroplast ultrastructure, antioxidant capacity, and growth of waterlogged maize seedlings. Sci Rep 9:484. https://doi.org/10.1038/s41598-018-36334-y

Santosh Kumar VV, Verma RK, Yadav SK, Yadav P, Watts A, Rao MV, Chinnusamy V (2020) CRISPR-Cas9 mediated genome editing of drought and salt tolerance (*OsDST*) gene in indica mega rice cultivar MTU1010. Physiol Mol Biol of Plants 26:1099–1110. https://doi.org/10.1007/s12298-020-00819-w

Satya Narayan V and Nair PM (1990) Metabolism, enzymology and possible roles of γ - amino butyrate in higher plants. Phytochemistry 29:367–375

Shelp BJ, Bown AW, McLean, MD (1999) Metabolism and functions of γ-aminobutyric acid. Trends Plant Sci 41:446–452

Shelp BJ, Mullen RT, Waller JC (2012a) Compartmentation of GABA metabolism raises intriguing questions. Trends Plant Sci 17:57–59.

Shelp BJ, Bozzo GG, Trobacher CP, Chiu G, Bajwa VS (2012b) Strategies and tool for studying the metabolism and function of aminobutyrate in plants. I. Pathway structure. Botany 90:651-668. https://doi.org/10.1139/b2012-041

Shimajiri Y, Oonishi T, Ozaki K, Kainou K, Akama K (2013a) Genetic manipulation of the γ-aminobutyric acid (GABA) shunt in rice: overexpression of truncated glutamate decarboxylase (*GAD2*) and knockdown of γ-aminobutyric acid transaminase (*GABA-T*) lead to sustained and high levels of GABA accumulation in rice kernels. Plant Biotechnol J 11:594–604. https://doi.org/10.1111/pbi.12050

Shimajiri Y, Ozaki K, Kainou K, Akama K (2013b) Differential subcellular localization, enzymatic properties and expression patterns of γ-aminobutyric acid transaminases (GABA-Ts) in rice (*Oryza sativa*). J Plant Physiol 170:196–201. https://doi.org/10.1016/j.jplph.2012.09.007

Sinha AK, Jaggi M, Raghuram B, Tuteja N. Mitogen-activated protein kinase signaling in plants under abiotic stress. Plant Signal Behav. 2011 Feb;6(2):196-203. https://doi.org/10.4161/psb.6.2.14701

Smith KT and Workman JL (2012) Chromatin proteins: key responders to stress. PLoS Biol 10(7):e1001371. https://doi.org/10.1371/journal.pbio.1001371

Snedden WA, Arazi T, Fromm T, Shelp BJ (1995) Calcium/calmodulin activation of soybean glutamate decarboxylase. Plant Physiol 108:543–549

Souza SC, Mazzafera P, Sodek L (2016) Flooding of the root system in soybean: biochemical and molecular aspects of N metabolism in the nodule during stress and recovery. Amino Acids 48 (5):1285–1295. https://doi.org/10.1007/s00726-016-2179-2

Steward FC, Thompson JF, Dent CE (1949) γ-aminobutyric acid: a constituent of the potato tuber? Science 110:439–440

Takayama M, Matsukura C, Ariizumi T, Ezura H (2017) Activating glutamate decarboxylase activity by removing the autoinhibitory domain leads to hyper γ-aminobutyric acid (GABA) accumulation in tomato fruit. Plant Cell Rep 36:103–116. https://doi.org/10.1007/s00299-016-2061-4

Tanaka H, Watanabe K, Ma M, Hirayama M, Kobayashi T, Oyama H, Sakaguchi Y, Kanda M, Kodama M, Aizawa Y (2009) The effects of gamma-aminobutyric acid, vinegar, and dried bonito on blood pressure in normotensive and mildly or moderately hypertensive volunteers. J Clin Biochem Nutr. 45:93–100. https://doi.org/10.3164/jcbn.09-04

Thitinunsomboon S, Keeratipibul S, Boonsiriwit A (2013) Enhancing gamma-aminobutyric acid content in germinated brown rice by repeated treatment of soaking and incubation. Food Sci Tech Intl 19:25-33. https://doi.org/10.1177/1082013212442180

Trobacher CP, Zarei A, Liu J, Clark SM, Bozzo GG, Shelp BJ (2013) Calmodulin- dependent and calmodulin-independent glutamate decarboxylases in apple fruit. BMC Plant Biol 13:144. https://doi.org/10.1186/1471-2229-13-144

Voytas, DF and Gao C (2014) Precision genome engineering and agriculture: opportunities and regulatory challenges. PLoS Biol 12:429–440. https://doi.org/10.1371/journal.pbio.1001877

Vridi AS, Singh S, Singh P (2015) Abiotic stress response in plants: roles of calmodulin - regulated proteins. Front Plant Sci 6: 809. https://doi.org/10.3389/fpls.2015.00809

Wang Y, Gu W, Meng Y, Xie T, Li L, Li J, Wei S (2017) γ-Aminobutyric acid imparts partial protection from salt stress injury to maize seedlings by improving photosynthesis and upregulating osmoprotectants and antioxidants. Sci Rep 7:43609. https://doi.org/10.1038/srep43609

Wani SH, Singh NB, Devi TR, Haribhushan A, Jeberson SM, Malik CP (2013). “Engineering abiotic stress tolerance in plants: extricating regulatory gene complex,” in

Conventional and Non-Conventional Interventions in Crop Improvement, eds C. P. Malik, G. S. Sanghera, and S. H. Wani (New Delhi: CABI), 1–19.

Wu Q, Su N, Huang X, Cui J, Shabala L, Zhou M, Yu M, Shabala S (2021) Hypoxia-induced increase in GABA content is essential for restoration of membrane potential and preventing ROS-induced disturbance to ion homeostasis. Plant Communs, 2(3), 00188. https://doi.org/10.1016/j.xplc.2021.100188

Wu X, Jia Q, Ji S, Gong B, Li J, Lu G, Gao H (2020) Gamma-aminobutyric acid (GABA) alleviates salt damage in tomato by modulating Na^+ uptake, the *GAD* gene, amino acid synthesis and reactive oxygen species metabolism. BMC Plant Biol 20: 465. https://doi.org/10.1186/s12870-020-02669-w

Xiang J, Chen X, Hu W, Xiang Y, Yan M, Wang J (2018) Overexpressing heat-shock protein OsHSP50. 2 improves drought tolerance in rice. Plant Cell Rep 37(11):1585–1595. https://doi.org/10.1007/s00299-018-2331-4

Yamakoshi J, Fukuda S, Satoh T, Tsuji R, Saito M, Obata A, Matsuyama A, Kikuchi M, Kawasaki, T (2007) Antihypertensive and natriuretic effects of less-sodium soy sauce containing γ-aminobutyric acid in spontaneously hypertensive rats. Biosci Biotechnol Biochem 71:165–173. https://doi.org/ 10.1271/bbb.60424

Yang H, Ren S, Yu S, Pan H, Li T, Ge S, Zhang J, Xia N (2020). Methods favoring homology-directed repair choice in response to CRISPR/Cas9 induced-double strand breaks. Int J Mol Sci 21, 6461. https://doi.org/10.3390/ijms21186461

Yang R, Yin Y, Gu Z (2015) Polyamine degradation pathway regulating growth and GABA accumulation in germinating Fava bean under hypoxia-NaCl stress. J Agril Sci Tech 17:311–320.

Yap KL, Yuan T, Mal TK, Vogel HJ, Ikura M (2003) Structural basis for simultaneous binding of two carboxy-terminal peptides of plant glutamate decarboxylase. J Mol Biol 328(1):193–204. https://doi.org/10.1016/S0022-2836(03)00271-7

Yong B, Xie H, Li Z, Li YP, Zhang Y, Nie G, Zhang XQ, Ma X, Huang LK, Yan YH (2017) Exogenous application of GABA improves PEG-induced drought tolerance positively associated with GABA-shunt, polyamines, and proline metabolism in white clover. Front Physiol 8:1107. https://doi.org/10.3389/fphys.2017.01107

Young M D, Wakefield M J, Smyth G K, Oshlack A (2010) Method Gene ontology analysis for RNA-seq: accounting for selection bias. Genome Biol 11: R14. https://doi.org/10.1186/gb-2010-11-2-r14

Zafar SA, Zaidi SSEA, Gaba Y, Singla-Pareek SL, Dhankher OP, Li X, Mansoor S, Pareek A (2020). Engineering abiotic stress tolerance via CRISPR/Cas-mediated genome editing. J Exp Bot 71:470–9. https://doi.org/10.1093/jxb/erz476

Zhang Y, Massel K, Godwin ID, Gao C (2018) Applications and potential of genome editing in crop improvement. Genome Biology 19:210. https://doi.org/10.1186/s13059-018-1586-y

Zhao G, Xie M, Wang Y, Li J (2017) Molecular Mechanisms Underlying γ-Aminobutyric Acid (GABA) accumulation in Giant Embryo Rice Seeds. J Agric Food Chem 65:4883−4889. https://doi.org/0.1021/acs.jafc.7b00013

Zhao Q and Dixon RA (2011) Transcriptional networks for lignin biosynthesis: More complex than we thought? Trends Plant Sci 16, 227–233. https://doi.org/10.1016/j.tplants.2010.12.005

Zheng Z, Zhang X, Liu J, He P, Zhang S, Zhang Y, Gao J, Yang S, Kang N, Afridi MI, Gao S, Chen C, Tu H (2021) GABAergic synapses suppress intestinal innate immunity via insulin signalling in Caenorhabditis elegans. Proc Natl Acad Sci USA. 118: e2021063118. https://doi.org/10.1073/pnas.2021063118

Zielinski RE (1998) Calmodulin and calmodulin-binding proteins in plants. Ann Rev Plant Physiol Plant Mol Biol 49:497–725. https://doi.org/10.1146/annurev.arplant.49.1.697